International Journal of Innovation and Applied Studies
ISSN 2028-9324 Vol. 12 No. 1 Jul. 2015, pp. 1-32

http://www.ijias.issr-journals.org/

Analytical solution of the peristaltic flow of a Jeffrey nanofluid in a tapered artery with mild stenosis and slip condition

Nabil T. M. El-dabe, Galal M. Moatimid, Mohamed A. Hassan, and Doaa R. Mostapha

Department of Mathematics, Faculty of Education,
Ain Shams University, Roxy, Cairo, Egypt

ABSTRACT: This paper investigates the effect of peristaltic flow of a Jeffrey nanofluid in endoscope. The flow is streaming through a tapered artery having a mild stenosis. The influences of heat and nanoparticle concentration on blood flow are also taken into account. Both velocity and thermal slip conditions are considered. The governing equations of motion, energy and nanoparticles are based on a perturbation technique. This technique depends on two parameters. Firstly, the amplitude ratio. Secondly, the small wave number. The distributions of the axial velocity, temperature and nanoparticle volume fraction are analytically derived. The pressure rise and friction force are numerically calculated. The numerical calculations are adopted to obtain the effects of several physical parameters, such as the slip parameter, Brownian motion parameter, thermophoresis parameter, the Reynolds number, the taper angle, nanoparticles Rayleigh number, thermal Rayleigh number and the maximum height of stenosis. It is found that the axial velocity increases with the decrease of the slip parameter. Meanwhile, it increases with the increase of both the nanoparticles Rayleigh number and the thermal Rayleigh number in the region of stenosis. The stream lines are also depicted. It is observed that the trapped bolus decreases in size with the increase of both the Brownian motion parameter and the thermophoresis parameter. In addition, the trapped bolus increases in size with the increase of both the maximum height of stenosis and the taper angle.

KEYWORDS: Peristaltic flow; Jeffrey model; Tapered artery; Stenosis flow; Nanoparticles; Slip condition; Heat transfer; Trapping phenomena.

1 INTRODUCTION

Several researches studied the non-Newtonian fluids because of their importance in industrial and technological applications. Such fluids have a nonlinear relationship between the stress and the rate of strain. Jeffrey model is considered as the simplest non-Newtonian fluid model. It is preferred to describe flow of physiological fluids in tubes and channels. Jeffrey model is a relatively linear model in which the time derivatives are used instead of convected derivatives. It has many industrial applications [1], such as notably polymer systems (melt and solutions) and multi-phase system such as foams, emulsions, and slurries. Also, we may considered it as a blood model. In recent years, several researchers have studied Jeffrey fluid under different conditions. Vajravelu et al. [2] investigated the peristaltic flow of a Jeffrey fluid in a vertical porous stratum with heat transfer under long wavelength and low Reynolds number assumptions. They found that the effects of the Jeffrey number, the Grashof number, the perturbation parameter, and the peristaltic wall deformation parameter have the strongest effects on the trapping bolus phenomenon. Furthermore, Lalitha Jyothi et al. [3] have considered the pulsatile flow of a Jeffrey fluid in a circular tube lined internally with porous material. They calculated the velocity and the flux of the fluid flow. Also, they found that the concentration is dragged towards the velocity profiles of the fluid flow in the tube.

The word "peristalsis" comes from a Greek word "Peristaltikos" which means clasping and compressing. Peristalsis is a well known mechanism for fluid transport in physiology. In this mechanism, sinusoidal waves travel on the walls of the tubes. It very useful in preventing the fluid from being contaminated over short distance. Furthermore, peristaltic has several

Corresponding Author: Mohamed A. Hassan

industrial applications [4], such as roller and finger pumps, nuclear industry for the transport of corrosive fluids, blood pump machine and heart lung machine. In addition, it is very important in biological mechanism which responsible for various physiological functions of the organs of the human body. It has many physiological activities [5], such as the transport of fluid through lymphatic vessels and transport deionized water and whole blood and deliver phosphated buffered saline into the vein of a rat. Also, the transport of urine from kidney to bladder, transport of food through oesophagus, the movement of eggs in the fallopian tube, transport of the spermatozoa in the cervical canal, transport of blood in heart, transport of bile in the bile duct are considered as another physiological applications. Several theoretical and experimental articles have been examined the peristaltic flows, such as Shapiro [6] and Manton [7]. Their works considered several assumptions, such as long wavelength approximation, low Reynolds number, small wave number and small amplitude ratio.

Blood flow in the artery has some important aspects due to the medical applications. It is a mixture of red cells, white cells and platelets in plasma. It is the bodily fluid which delivers nutrient and oxygen to the cells and transport waste products away. The hemodynamic behavior of the blood flow is influenced by the presence of arterial stenosis. A stenosis is the abnormal growth of tissue. Stenosis means narrowing of any body passage [8]. stenoses may be caused by the impingement of extra vascular masses. Also, it may be formed due to intravascular atherosclerotic plaques which develop at the wall of the artery and protrude into the lumen. It may leads to blood clot, cerebral strokes or heart attack, myocardial infarction and heart failure by reducing or occluding the blood supply [9]. Furthermore, stenosis may damage the internal cells of the wall. Several efforts have been made to investigate the blood flow characteristics through stenosed arteries. Chakravarty et al. [10] investigated the problem of nonlinear blood flow in a stenosed flexible artery. Also, Verma and Parihar [11] discussed the mathematical model of blood flow through a tapered artery with mild stenosis.

Heat transfer analysis is one of the important topic in industrial research and studying chemical engineering. It is the passage of thermal energy from a hot body to a colder one. Bio-heat is considered as heat transfer in human body. It includes thermotherapy and human thermoregulation system [12]. The thermotherapy system is on of the most important application of heat in the human body. The applications of heat (hyperthermia), radiation (laser therapy) and coldness (cryosurgery) help to destroy undesirable tissues including cancer. In physiology, heat transfer is used to study the properties of tissues. The processes of oxygenation and hemodialysis have also been visualized by considering peristaltic flows with heat transfer. Peristaltic flow with heat transfer has many applications in biomedical sciences and industry such as conduction in tissues, heat convection due to blood flow from the pores of tissues, radiation between environment and its surface, food processing and vasodilation. Furthermore, it used to generate metabolic heat and heat transfer due to some external interactions such as, mobile phones and radioactive treatments. Also, convection is seen in the ocean currents, sea-wind formation, rising of plume of hot air from fire, formation of micro-structres during the cooling of molten metals, solar ponds and in fluid flows around heat dissipation fins. The application radio-frequency therapy is important to treat more diseases such as tissue coagulation, the primary liver cancer, the lung cancer and the reflux of stomach acid [13]. Many investigators have reported the influence of heat transfer on peristaltic flow of Newtonian and non-Newtonian fluids. Nadeem and Akbar [14] studied the influence of heat transfer on a peristaltic transport of Herschel-Bulkley fluid in a non uniform inclined tube.

In the last decades, the study of nanofluid is an important area which has attracted the attention of many investigators. Fluids with nano-scaled particles interaction are called as nanofluid. Nanofluids refer to heat transfer liquids with enhanced heat transfer capability. Nanofluid is defined as the study of fluid flow in and around nono-sized objects. Furthermore, it is a new class of fluids designed by dispersing nanometer-sized materials, such as nanoparticles, nanofibers, nanotubes, nanowires, nanorods, nanosheet and droplets, in base fluids. The nonoparticles used in nanofluid are normally composed of metals, oxides, carbides or carbon nanotubes. Water, ethylene glycol and engine oil are common examples of base fluids. The first investigation of the nanofluid was introduced by Choi [15] . Choi [15] reported that an innovative technique to improve heat transfer is done by using nano-scale particles in the base fluid. Further, Choi et al. [16] showed that the addition of a small amount of nanoparticles to conventional heat transfer liquids increased the thermal conductivity of the fluid up to approximately two times. Nanofluids have major applications in heat transfer, including microelectronics, fuel cells, pharmaceutical processes, hybrid-powered engines, domestic refrigerator, chiller, nuclear reactor coolant, grinding and space technology. Also, there are another activities of nanofluids, such as boiler flue gas temperature reduction, biological organisms, snapping shrimps, super-hydrophobic beetle wings and use of charged polymers for lubrication. In addition, the lotus effect for self-cleaning surfaces, membranes for filtering on size or charge (e.g. for desalination), nanoporous materials for size exclusion chromatography, passive selective transport in aquaporins, active transport in ion channels, molecular motors like kinesis and charge based filtration in the kidney basal membrane are considered the important applications of nanofluids [17].

In the cancer treatment, magnetic nanoparticles are injected into the blood vessel nearest to the cancer's tissues. The dynamic of these nanoparticles occurs under the action of the peristaltic waves generated on the flexible walls of the blood vessel. Studying such nanofluid flow under this action is, therefore, useful in treating tissues of the cancer. Mekheimer and

Abd elmaboud [18] found that the tissues of cancer are destroyed if the temperature reaches $42-45^{\circ}$C. On the other hand, in this application the drug may be placed on the magnetic nanoparticles and is injected near the tumor. Then, the drug is absorbed by the tumor through a high gradient magnetic field, which is concentrated near the tumor center [19]. Therefore, the interaction of nanoparticles in peristaltic flows has now been receiving attentions of many researchers. Akram et al. [20] investigated the influence of peristaltic transport on Jeffrey nonofluid in an asymmetric channel. Also, Ebid and Aly [21] studied the peristaltic nanofluids flow in a channel with flexible walls and slip condition. This study was considered as an application to the cancer treatment. Furthermore, many investigators studied the interaction between nanoparticles and mild stenosis. Ellahi et al. [22] investigated the blood flow of nanofluid with stenosis and permeable walls. Also, the problem of blood flow in the nano-Prandtl fluid of tapered stenosed arteries has been discussed by Nadeem et al.[23].

The effect of vessel tapering is an important factor in studying peristaltic transport. Pandey and Chaube [24] studied the axi-symmetric peristaltic transport of a viscous incompressible viscoelastic fluid through a circular tube whose cross section changes along the length (tapered tube). The Newtonian and non-Newtonian blood flow through tapered arteries with a stenosis have been investigated. Mandal [25] studied the notable characteristics of the non-Newtonian blood flow (Power-law model) through a flexible tapered arteries in the presence of stenosis subject to the pulsatile pressure gradient. Also, Akbar et al. [26] discussed the theoretical study of nanofluid flow through composite stenosed arteries. In studying the peristaltic flow, many researches assumed that the fluid layer next to the surface moves with it, which is so called no slip condition. However, there are another works that considered hypotheses including slippage. The so called slip conditions means that there is a relative motion between the fluid layer next to the fluid surface. It states that the velocity of the fluid at the plate is linearly proportional to the shear stress at this plate [27]. It is very important in the polishing of artificial heart valves. Also, it is important for internal cavities in a variety of manufactured parts, micro-channels or nano-channels. The slip condition plays a vital role in shear skin spurt and hysteresis effects. Furthermore, the fluids that exhibit boundary slip have essential technological applications when a thin film of light oil is attached to the moving plates. Also, it is used when the surface is coated with a special coating such as a thick monolayer. The problem of effects of magnetic field and wall slip conditions on the peristaltic transport of a Newtonian fluid in an asymmetric channel was discussed by Ebaid [28]. Also, Abbasi et al. [29] investigated peristaltic transport of copper-water nanofluid in an inclined channel in the presence of velocity and thermal slip conditions.

From the motivation of above discussion, the aim of the present study aims to investigate the effect of heat transfer on peristaltic flow of Jeffrey nanofluid in a vertical annulus. The flow is streaming through a tapered artery with mild stenosis. Furthermore, the influences of slip conditions of velocity, heat and nanoparticles are also considered. The governing equations of motion, energy and nanoparticle volume fraction are based on a perturbation technique. This technique depends on two parameters. Firstly, the amplitude ratio. Secondly, the small wave number. These equations are analytically solved in accordance with the appropriate boundary conditions. The pressure rise and friction force are obtained in terms of dimensionless flow rate Q by using numerical integration. Numerical calculations are adopted to obtain the effects of several parameters, such as the Reynolds number, the slip parameters, Brownian motion parameter, thermophoresis parameter, the taper angle, nanoparticles Rayleigh number, thermal Rayleigh number, the ratio of relaxation to retardation times and the maximum height of stenosis. As a special case of this study, when the previous parameters tend to zero, the results reduce to the same as that found by Fung and Yih [30]. To clarify the problem at hand, in section 2, the physical description of the problem including the basic equations governing the motion with the appropriate boundary conditions are presented. Section 3 is devoted to introduce the method of solution according to a perturbation technique. Through section 4, we introduce some important results that are displayed graphically for pumping characteristics and trapping phenomena. Finally, in section 5, we give concluding remarks based on the obtained results for peristaltic transport and stream lines.

2 FORMULATION OF THE PROBLEM

Consider an unsteady Jeffrey fluid through vertical annulus. The outer tube is tapered and has a sinusoidal wave traveling down its wall with mild stenosis. The inner one is rigid, uniform, and moving with a uniform velocity V_0. The cylindrical polar co-ordinates system (r, θ, z) are used, so that the z-axis lies along the centerline of the inner and outer tubes. Through this study, we consider the case of an axial symmetry. In other word, non of any physical quantities depend on the coordinates θ. The gravitational acceleration g is also taken into account. The inner and outer tubes are located at $r = r_1$ and $r = R(z) + h_1$, respectively. They are maintained at the uniform temperatures T_0 and T_1, respectively. Also, they are maintained at the uniform nanoparticles concentration C_0 and C_1, respectively. The slip conditions are also considered.

The effective radius of the outer tube $R(z)$ [11] is taken as follows:

$$R(z)=\begin{cases} R_1-m(z+L) & \mathrm{L}<\mathrm{z}<-\mathrm{z}_0, \\ R_1-m(z+L)-\dfrac{H}{2}[1+\cos\dfrac{\pi z}{z_0}] & -\mathrm{z}_0\le \mathrm{z}\le \mathrm{z}_0, \\ R_1-m(z+L) & \mathrm{z}_0<\mathrm{z}<\mathrm{d}, \end{cases} \tag{1}$$

where $R(z)$ is the effective radius of the tapered artery, R_1 is the radius of the un-tapered outer tube, $H=h\cos\phi$ is the hight of the stenosis in the tapered artery, ϕ is the angle of tapering, h is the maximum hight of the stenosis, z_0 is the half-length of the stenosis and $m=\tan\phi$ is the slope of the tapered vessel. Sketch of the problem is given in the figure 1.

The ratio between the height of the stenosis and the radius of the normal artery is much less than unity. The arterial is taken to be of finite length $L+d$ [10]. This study focus on all possibilities of different shapes of the artery viz, the converging tapering $\phi<0$, non-tapered artery $\phi=0$ and the diverging tapering $\phi>0$ [25].

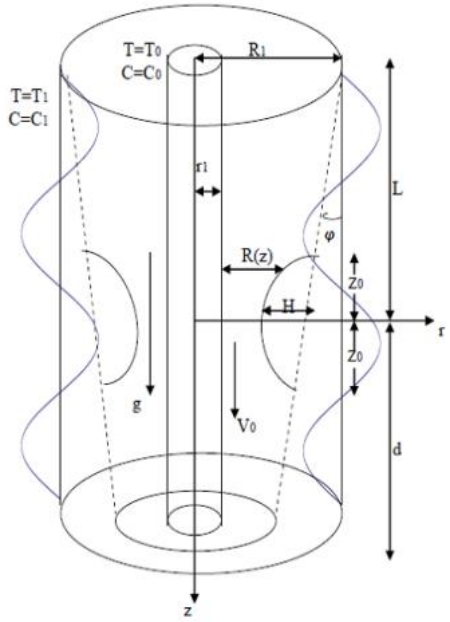

Fig. 1. Sketch of the physical situation of the problem

The prototype of fluid designed by Jeffrey is considered. Therefore, the constitutive equation is then become [1]

$$\underline{S}=\frac{\mu}{1+\lambda_1}\left(\underline{A}+\lambda_2\underline{\dot{A}}\right), \tag{2}$$

where $\underline{S}$ is the stress deviator, μ is dynamic viscosity, λ_1 is the ratio of the relaxation time to retardation one, λ_2 is the retardation time,

$$\underline{A}=L+L^T, \tag{3}$$

is the rate of strain tensor, (dot) denotes the differentiation with respect to time, $\underline{V}=(u,0,w)$ is the velocity field and $L=\nabla\underline{V}$.

Since we assume that the base fluid density ρ_f is uniform, it follows that the incompressibility condition is then become

$$\nabla.\underline{V}=0. \tag{4}$$

The equation of motion may be written as

$$\rho\left(\frac{\partial \underline{V}}{\partial t}+(\underline{V}.\nabla)\underline{V}\right)=-\nabla p+\nabla.\underline{S}+\rho\underline{g}, \tag{5}$$

where p is the pressure and $\underline{g}=(0,0,g)$.

The density for the nanofluids is [31]

$$\rho=C\rho_p+(1-C)\rho_f\left(1-B_t(T-T_0)\right), \tag{6}$$

where C is the nanoparticle volume fraction of the nanofluid, ρ_p is the density of the nanoparticles, ρ_p is the density of the fluid, B_t is the volumetric expansion coefficient of the nanofluid and T is the temperature.

The equation of energy [20] is given by

$$(\rho c)_f\left(\frac{\partial T}{\partial t}+\underline{V}.\nabla T\right)=K\nabla^2T+(\rho c)_p\left(D_B\nabla C.\nabla T+\frac{D_T}{T_0}\nabla T.\nabla T\right), \tag{7}$$

where T is the temperature, $k=\dfrac{K}{(\rho c)_f}$ is the thermometric conductivity, K is the thermal conductivity, c_f is the specific heat of the base fluid, c_p is the specific heat of the nanoparticles, D_B is the Brownian diffusion coefficient and D_T is the thermophoretic diffusion coefficient.

The equation of nanoparticle volume fraction in the nanofluid [20] is given by

$$\frac{\partial C}{\partial t}+\underline{V}.\nabla C=D_B\nabla^2C+\frac{D_T}{T_0}\nabla^2T. \tag{8}$$

The geometry of the peristaltic wall surface is defined as [6]

$$h_1=a\cos\frac{2\pi}{\lambda}\left(z-\frac{kt}{R_1}\right), \tag{9}$$

where a is the wave amplitude, λ is the wave length and $\dfrac{kt}{R_1}$ is the wave speed.

The appropriate boundary conditions may be listed as follows [[21] and [30]]:

$$u=\frac{\partial h_1}{\partial t},\quad w=-\gamma S_{rz},\quad T+\eta\frac{\partial T}{\partial r}=T_1,\quad C+\beta\frac{\partial C}{\partial r}=C_1\quad at\quad r_2=R(z)+h_1, \tag{10}$$

$$u=0,\quad w=V_0,\quad T=T_0,\quad C=C_0\quad at\quad r=r_1, \tag{11}$$

where γ is the velocity slip parameter, η is the thermal slip parameter and β is the slip parameter of nanoparticle volume fraction.

Combining Eqs. (2), (3) and (6), the r and z -components of the Eq. of motion (5) may be written as follows:

r -component:

$$\rho_f\left(\frac{\partial u}{\partial t}+u\frac{\partial u}{\partial r}+w\frac{\partial u}{\partial z}\right)=-\frac{\partial p}{\partial r}+\frac{2\mu}{1+\lambda_1}\left[\frac{1}{r}\frac{\partial u}{\partial r}+\frac{\partial^2u}{\partial r^2}+\frac{1}{2}\frac{\partial^2u}{\partial z^2}+\frac{1}{2}\frac{\partial^2w}{\partial r\partial z}\right.$$

$$-\frac{u}{r^2}+\lambda_2\left(\frac{1}{r}\frac{\partial^2u}{\partial r\partial t}+\frac{\partial^3u}{\partial r^2\partial t}+\frac{1}{2}\frac{\partial^3u}{\partial z^2\partial t}+\frac{1}{2}\frac{\partial^3w}{\partial r\partial z\partial t}-\frac{1}{r^2}\frac{\partial u}{\partial t}+\frac{u}{r}\frac{\partial^2u}{\partial r^2}+U\frac{\partial^3u}{\partial r^3}\right.$$

$$\left.\left.+\frac{1}{2}u\frac{\partial^3u}{\partial r\partial z^2}+\frac{1}{2}u\frac{\partial^3w}{\partial r^2\partial z}-\frac{u}{r^2}\frac{\partial u}{\partial r}+\frac{u^2}{r^3}+\frac{w}{r}\frac{\partial^2u}{\partial r\partial z}+w\frac{\partial^3u}{\partial r^2\partial z}+\frac{1}{2}w\frac{\partial^3u}{\partial z^3}\right.\right.$$

$$+\frac{1}{2}w\frac{\partial^3 w}{\partial z^2\partial r}-\frac{w}{r^2}\frac{\partial u}{\partial z}+\frac{\partial u}{\partial r}\frac{\partial^2 u}{\partial r^2}+\frac{\partial w}{\partial r}\frac{\partial^2 u}{\partial r\partial z}+\frac{1}{2}\frac{\partial u}{\partial z}\frac{\partial^2 u}{\partial r\partial z}+\frac{1}{2}\frac{\partial u}{\partial z}\frac{\partial^2 w}{\partial r^2}$$

$$+\frac{1}{2}\frac{\partial w}{\partial z}\frac{\partial^2 u}{\partial z^2}+\frac{1}{2}\frac{\partial w}{\partial z}\frac{\partial^2 w}{\partial r\partial z})], \tag{12}$$

z -component:

$$\rho_f(\frac{\partial w}{\partial t}+u\frac{\partial w}{\partial r}+w\frac{\partial w}{\partial z})=-\frac{\partial p}{\partial z}+\frac{\mu}{1+\lambda_1}[\frac{1}{r}\frac{\partial u}{\partial z}+\frac{1}{r}\frac{\partial w}{\partial r}+\frac{\partial^2 u}{\partial z\partial r}+\frac{\partial^2 w}{\partial r^2}$$

$$+2\frac{\partial^2 w}{\partial z^2}+\lambda_2(\frac{1}{r}\frac{\partial^2 U}{\partial z\partial t}+\frac{1}{r}\frac{\partial^2 w}{\partial r\partial t}+\frac{\partial^3 u}{\partial z\partial r\partial t}+\frac{\partial^3 w}{\partial r^2\partial t}+2\frac{\partial^3 w}{\partial z^2\partial t}+\frac{u}{r}\frac{\partial^2 u}{\partial r\partial z}$$

$$+\frac{u}{r}\frac{\partial^2 w}{\partial r^2}+u\frac{\partial^3 u}{\partial r^2\partial z}+u\frac{\partial^3 w}{\partial r^3}+2u\frac{\partial^3 w}{\partial r\partial z^2}+\frac{w}{r}\frac{\partial^2 u}{\partial z^2}+\frac{w}{r}\frac{\partial^2 w}{\partial r\partial z}+w\frac{\partial^3 u}{\partial z^2\partial r}$$

$$+w\frac{\partial^3 w}{\partial r^2\partial z}+2w\frac{\partial^3 w}{\partial z^3}+\frac{\partial u}{\partial r}\frac{\partial^2 u}{\partial r\partial z}+\frac{\partial u}{\partial r}\frac{\partial^2 w}{\partial r^2}+\frac{\partial w}{\partial r}\frac{\partial^2 u}{\partial z^2}+\frac{\partial w}{\partial r}\frac{\partial^2 w}{\partial r\partial z}$$

$$+2\frac{\partial u}{\partial z}\frac{\partial^2 w}{\partial r\partial z}+2\frac{\partial w}{\partial z}\frac{\partial^2 w}{\partial z^2})]+C\rho_p g+(1-C)\rho_f[1-B_t(T-T_0)]g, \tag{13}$$

the continuity equation

$$\frac{1}{r}\frac{\partial(ru)}{\partial r}+\frac{\partial w}{\partial z}=0. \tag{14}$$

and the Eq. of energy (7) may be written as follows:

$$\frac{\partial T}{\partial t}+u\frac{\partial T}{\partial r}+w\frac{\partial T}{\partial z}=\tau\left(D_B\left(\frac{\partial T}{\partial r}\frac{\partial C}{\partial r}+\frac{\partial T}{\partial z}\frac{\partial C}{\partial z}\right)+\frac{D_T}{T_0}\left((\frac{\partial T}{\partial r})^2+(\frac{\partial T}{\partial z})^2\right)\right)$$

$$+K\left(\frac{\partial^2 T}{\partial r^2}+\frac{1}{r}\frac{\partial T}{\partial r}+\frac{\partial^2 T}{\partial z^2}\right), \tag{15}$$

where $\tau=\frac{(\rho c)_p}{(\rho c)_f}$ is the ratio between the effective heat capacity of the nanoparticles material and the effective heat capacity of the base fluid.

Finally, the equation of nanoparticle volume fraction in the nanofluid (8) may be written as follows:

$$\frac{\partial C}{\partial t}+u\frac{\partial C}{\partial r}+w\frac{\partial C}{\partial z}=D_B\left(\frac{\partial^2 C}{\partial r^2}+\frac{1}{r}\frac{\partial C}{\partial r}+\frac{\partial^2 C}{\partial z^2}\right)+\frac{D_T}{T_0}\left(\frac{\partial^2 T}{\partial r^2}+\frac{1}{r}\frac{\partial T}{\partial r}+\frac{\partial^2 T}{\partial z^2}\right). \tag{16}$$

The instantaneous volume flow rate is defined as:

$$Q=2\pi\int_{r_1}^{r_2}wrdr, \tag{17}$$

where R_2 is a function of z and t.

The time averaged $\hat{Q}$ (time mean flow) over period $\tau=\frac{\lambda R_1}{k}$ is defined as

$$\hat{Q}=\frac{1}{\tau}\int_0^{\tau}Q d\tau. \tag{18}$$

In this analysis, we consider the stream function $\psi=\psi(r,z,t)$ which may be expressed as

$$u=\frac{1}{r}\frac{\partial\psi}{\partial z},\quad \text{and}\quad w=-\frac{1}{r}\frac{\partial\psi}{\partial r}. \tag{19}$$

Combining Eqs. (10-16), one gets:

r-component:

$$\rho_f\left(\frac{1}{r}\frac{\partial^2\psi}{\partial z\partial t}+\frac{1}{r}\frac{\partial\psi}{\partial z}(-\frac{1}{r^2}\frac{\partial\psi}{\partial z}+\frac{1}{r}\frac{\partial^2\psi}{\partial r\partial z})-\frac{1}{r^2}\frac{\partial\psi}{\partial r}\frac{\partial^2\psi}{\partial z^2}\right)=-\frac{\partial p}{\partial r}+\frac{2\mu}{1+\lambda_1}(-\frac{1}{2r^2}\frac{\partial^2\psi}{\partial r\partial z}$$

$$+\frac{1}{2r}\frac{\partial^3\psi}{\partial r^2\partial z}+\frac{1}{2r}\frac{\partial^3\psi}{\partial z^3}+\lambda_2[-\frac{1}{2r^2}\frac{\partial^3\psi}{\partial r\partial z\partial t}+\frac{1}{2r}\frac{\partial^4\psi}{\partial r^2\partial z\partial t}+\frac{1}{2r}\frac{\partial^4\psi}{\partial z^3\partial t}+\frac{1}{r}\frac{\partial\psi}{\partial z}(-\frac{4}{r^4}\frac{\partial\psi}{\partial z}$$

$$+\frac{6}{r^3}\frac{\partial^2\psi}{\partial r\partial z}-\frac{2}{r^2}\frac{\partial^3\psi}{\partial r^2\partial z}+\frac{1}{2r}\frac{\partial^4\psi}{\partial r^3\partial z}+\frac{1}{2r}\frac{\partial^4\psi}{\partial r\partial z^3}-\frac{1}{2r^2}\frac{\partial^3\psi}{\partial z^3})-\frac{1}{r}\frac{\partial\psi}{\partial r}(-\frac{3}{2r^2}\frac{\partial^3\psi}{\partial z^2\partial r}$$

$$+\frac{1}{2r}\frac{\partial^4\psi}{\partial r^2\partial z^2}+\frac{1}{2r}\frac{\partial^4\psi}{\partial z^4}+\frac{2}{r^3}\frac{\partial^2\psi}{\partial z^2})-\frac{5}{2r^3}(\frac{\partial^2\psi}{\partial r\partial z})^2+\frac{3}{2r^2}\frac{\partial^2\psi}{\partial r\partial z}\frac{\partial^3\psi}{\partial r^2\partial z}+\frac{2}{r^3}\frac{\partial^2\psi}{\partial r^2}\frac{\partial^2\psi}{\partial z^2}$$

$$-\frac{1}{r^2}\frac{\partial^2\psi}{\partial r^2}\frac{\partial^3\psi}{\partial z^2\partial r}+\frac{1}{2r^2}\frac{\partial^2\psi}{\partial z^2}\frac{\partial^3\psi}{\partial z^2\partial r}-\frac{1}{2r^2}\frac{\partial^2\psi}{\partial z^2}\frac{\partial^3\psi}{\partial r^3}-\frac{1}{2r^2}\frac{\partial^2\psi}{\partial r\partial z}\frac{\partial^3\psi}{\partial z^3}-\frac{1}{2r^3}(\frac{\partial^2\psi}{\partial z^2})^2]), \tag{20}$$

z-component:

$$\rho_f\left(-\frac{1}{r}\frac{\partial^2\psi}{\partial r\partial t}+\frac{1}{r}\frac{\partial\psi}{\partial z}(\frac{1}{r^2}\frac{\partial\psi}{\partial r}-\frac{1}{r}\frac{\partial^2\psi}{\partial r^2})+\frac{1}{r^2}\frac{\partial\psi}{\partial r}\frac{\partial^2\psi}{\partial z\partial r}\right)=-\frac{\partial p}{\partial z}+\frac{\mu}{1+\lambda_1}(-\frac{1}{r^3}\frac{\partial\psi}{\partial r}$$

$$+\frac{1}{r^2}\frac{\partial^2\psi}{\partial r^2}-\frac{1}{r}\frac{\partial^3\psi}{\partial r^3}-\frac{1}{r}\frac{\partial^3\psi}{\partial z^2\partial r}+\lambda_2[-\frac{1}{r^3}\frac{\partial^2\psi}{\partial r\partial t}+\frac{1}{r^2}\frac{\partial^3\psi}{\partial r^2\partial t}-\frac{1}{r}\frac{\partial^4\psi}{\partial z^2\partial r\partial t}-\frac{1}{r}\frac{\partial^4\psi}{\partial r^3\partial t}$$

$$+\frac{1}{r}\frac{\partial\psi}{\partial z}(\frac{2}{r^3}\frac{\partial^2\psi}{\partial z^2}-\frac{1}{r}\frac{\partial^4\psi}{\partial r^2\partial z^2}+\frac{6}{r^4}\frac{\partial\psi}{\partial r}-\frac{6}{r^3}\frac{\partial^2\psi}{\partial r^2}+\frac{3}{r^2}\frac{\partial^3\psi}{\partial r^3}-\frac{1}{r}\frac{\partial^4\psi}{\partial r^4})-\frac{1}{r}\frac{\partial\psi}{\partial r}(-\frac{1}{r^2}\frac{\partial^3\psi}{\partial z^3}$$

$$+\frac{2}{r^2}\frac{\partial^3\psi}{\partial r^2\partial z}-\frac{1}{r}\frac{\partial^4\psi}{\partial r\partial z^3}-\frac{1}{r}\frac{\partial^4\psi}{\partial r^3\partial z})+\frac{1}{r^3}\frac{\partial^2\psi}{\partial r\partial z}\frac{\partial^2\psi}{\partial z^2}+\frac{3}{r^2}\frac{\partial^2\psi}{\partial r\partial z}\frac{\partial^3\psi}{\partial z^2\partial r}+\frac{1}{r^3}\frac{\partial^2\psi}{\partial r^2}\frac{\partial^2\psi}{\partial z\partial r}$$

$$-\frac{1}{r^2}\frac{\partial^3\psi}{\partial r^3}\frac{\partial^2\psi}{\partial z\partial r}-\frac{1}{r^2}\frac{\partial^2\psi}{\partial r^2}\frac{\partial^3\psi}{\partial z^3}-\frac{2}{r^2}\frac{\partial^2\psi}{\partial z^2}\frac{\partial^3\psi}{\partial r^2\partial z}+\frac{1}{r^2}\frac{\partial^2\psi}{\partial r^2}\frac{\partial^3\psi}{\partial r^2\partial z}])+C\rho_p g+(1-C)$$

$$\times\rho_f[1-B_t(T-T_0)]g. \tag{21}$$

Eq. of energy may be written as follows:

$$\frac{\partial T}{\partial t}+\frac{1}{r}\frac{\partial\psi}{\partial z}\frac{\partial T}{\partial r}-\frac{1}{r}\frac{\partial\psi}{\partial r}\frac{\partial T}{\partial z}=\tau\left(D_B\left(\frac{\partial T}{\partial r}\frac{\partial C}{\partial r}+\frac{\partial T}{\partial z}\frac{\partial C}{\partial z}\right)+\frac{D_T}{T_0}\left((\frac{\partial T}{\partial r})^2+(\frac{\partial T}{\partial z})^2\right)\right)$$

$$+K\left(\frac{\partial^2 T}{\partial r^2}+\frac{1}{r}\frac{\partial T}{\partial r}+\frac{\partial^2 T}{\partial z^2}\right). \tag{22}$$

Also, Eq. of nanoparticle volume fraction in the nanofluid may be written as follows:

$$\frac{\partial C}{\partial t}+\frac{1}{r}\frac{\partial \psi}{\partial z}\frac{\partial C}{\partial r}-\frac{1}{r}\frac{\partial \psi}{\partial r}\frac{\partial C}{\partial z}=D_B\left(\frac{\partial^2 C}{\partial r^2}+\frac{1}{r}\frac{\partial C}{\partial r}+\frac{\partial^2 C}{\partial z^2}\right)+\frac{D_T}{T_0}\left(\frac{\partial^2 T}{\partial r^2}+\frac{1}{r}\frac{\partial T}{\partial r}+\frac{\partial^2 T}{\partial z^2}\right), \tag{23}$$

and the boundary conditions (10) and (11) take the following forms:

$$\frac{\partial \psi}{\partial r}=r\gamma S_{rz},\quad \frac{\partial \psi}{\partial z}=\frac{2\pi akr}{\lambda R_1}\sin\frac{2\pi}{\lambda}\left(z-\frac{k}{R_1}t\right),\quad T+\eta\frac{\partial T}{\partial r}=T_1,\quad C+\beta\frac{\partial C}{\partial r}=C_1\quad at\quad r_2=R(z)+h_1, \tag{24}$$

$$\frac{\partial \psi}{\partial z}=0,\quad -\frac{1}{r}\frac{\partial \psi}{\partial r}=V_0,\quad T=T_0\quad \text{and}\quad C=C_0\quad at\quad r=r_1. \tag{25}$$

It is convenient to write the forgoing equations in an appropriate dimensionless form. This can be done in a number of ways depending primarily on the choice of the characteristic length, time, and mass. Consider the following dimensionless forms depending on the characteristic length R_1, the characteristic time $\frac{R_1^2}{k}$ and the characteristic mass M. The other dimensionless quantities are given by

$$\bar{r}=\frac{r}{R_1},\quad \bar{z}=\frac{z}{R_1},\quad \bar{u}=\frac{uR_1}{k},\quad \bar{w}=\frac{wR_1}{k},\quad \bar{h_1}=\frac{h_1}{R_1},\quad \delta=\frac{R_1}{\lambda}$$

$$\bar{S}=\frac{SR_1^2}{\mu k},\quad \bar{z_0}=\frac{z_0}{R_1},\quad \bar{L}=\frac{L}{R_1},\quad \bar{d}=\frac{d}{R_1},\quad \bar{h}=\frac{h}{R_1},\quad \overline{R(z)}=\frac{R(z)}{R_1},$$

$$\bar{\psi}=\frac{\psi}{kR_1},\quad \bar{p}=\frac{pR_1^2}{\rho_f k},\quad \bar{\theta}=\frac{T-T_0}{T_1-T_0},\quad \bar{\sigma}=\frac{C-C_0}{C_1-C_0}\quad \text{and}\quad \bar{Q}=\frac{Q}{2\pi R_1 k}. \tag{26}$$

On using the above dimensionless quantities in the forgoing equations of motion, these quantities will be arised in a dimensionless forms including the following dimensionless parameters: $R_N=\frac{R_1^3(C_1-C_0)g(\rho_p-\rho_f)}{\rho_f k^2}$ is the nanoparticles Rayleigh number or the nanoparticles Grashof number, $R_a=\frac{R_1^3(1-C_0)B_t(T_1-T_0)g}{\mu k^2}$ is the thermal Rayleigh number or the local temperature Grashof number, $R_M=\frac{R_1^3 g(\rho_p C_0+(1-C_0)\rho_f)}{\rho_f k^2}$ is basic density Rayleigh number, $\varepsilon=a/R_1$ is the amplitude ratio, $\alpha=\frac{2\pi R_1}{\lambda}$ is the wave number, $N_b=\frac{\tau D_B(C_1-C_0)}{k}$ is the Brownian motion parameter, $N_t=\frac{\tau D_T(T_1-T_0)}{kT_0}$ is the thermophoresis parameter, $\Lambda_2=\frac{\lambda_2 k}{R_1^2}$ is the Weissenberg number, $R_e=\frac{\rho_f k}{\mu}$ is the Reynolds number, $\gamma^*=\frac{\gamma\mu}{R_1}$ is Kudsen number or non-dimensional velocity slip parameter, $\eta^*=\frac{\eta}{R_1}$ is the non-dimensional thermal slip parameter, $\beta^*=\frac{\beta}{R_1}$ is the non-dimensional slip parameter of nanoparticle volume fraction and $V_0^*=\frac{V_0R_1}{k}$. The bars mark refer to the dimensionless quantities. From now on, these will be omitted for simplicity.

The dimensionless effective radius of the tube $R(z)$ becomes:

$$R(z)=\begin{cases} R_1-m(z+L) & \mathrm{L}<\mathrm{z}<-\mathrm{z}_0, \\ R_1-m(z+L)-\dfrac{H}{2}[1+\cos\dfrac{\pi z}{z_0}] & -\mathrm{z}_0\le \mathrm{z}\le \mathrm{z}_0, \\ R_1-m(z+L) & \mathrm{z}_0<\mathrm{z}<\mathrm{d}, \end{cases} \tag{27}$$

The dimensionless governing equations (20)-(25) may be rewritten as:

r-component:

$$\frac{1}{r}\frac{\partial^2\psi}{\partial z\partial t}+\frac{1}{r}\frac{\partial\psi}{\partial z}(-\frac{1}{r^2}\frac{\partial\psi}{\partial z}+\frac{1}{r}\frac{\partial^2\psi}{\partial r\partial z})-\frac{1}{r^2}\frac{\partial\psi}{\partial r}\frac{\partial^2\psi}{\partial z^2}=-\frac{\partial p}{\partial r}+\frac{1}{R_e(1+\lambda_1)}(-\frac{1}{r^2}\frac{\partial^2\psi}{\partial r\partial z}$$
$$+\frac{1}{r}\frac{\partial^3\psi}{\partial r^2\partial z}+\frac{1}{r}\frac{\partial^3\psi}{\partial z^3}+\Lambda_2[-\frac{1}{r^2}\frac{\partial^3\psi}{\partial r\partial z\partial t}+\frac{1}{r}\frac{\partial^4\psi}{\partial r^2\partial z\partial t}+\frac{1}{r}\frac{\partial^4\psi}{\partial z^3\partial t}+\frac{1}{r}\frac{\partial\psi}{\partial z}(-\frac{8}{r^4}\frac{\partial\psi}{\partial z}$$
$$+\frac{12}{r^3}\frac{\partial^2\psi}{\partial r\partial z}-\frac{4}{r^2}\frac{\partial^3\psi}{\partial r^2\partial z}+\frac{1}{r}\frac{\partial^4\psi}{\partial r^3\partial z}+\frac{1}{r}\frac{\partial^4\psi}{\partial r\partial z^3}-\frac{1}{r^2}\frac{\partial^3\psi}{\partial z^3})-\frac{1}{r}\frac{\partial\psi}{\partial r}(-\frac{3}{r^2}\frac{\partial^3\psi}{\partial z^2\partial r}$$
$$+\frac{1}{r}\frac{\partial^4\psi}{\partial r^2\partial z^2}+\frac{1}{r}\frac{\partial^4\psi}{\partial z^4}+\frac{4}{r^3}\frac{\partial^2\psi}{\partial z^2})-\frac{5}{r^3}(\frac{\partial^2\psi}{\partial r\partial z})^2+\frac{3}{r^2}\frac{\partial^2\psi}{\partial r\partial z}\frac{\partial^3\psi}{\partial r^2\partial z}+\frac{4}{r^3}\frac{\partial^2\psi}{\partial r^2}\frac{\partial^2\psi}{\partial z^2}$$
$$-\frac{2}{r^2}\frac{\partial^2\psi}{\partial r^2}\frac{\partial^3\psi}{\partial z^2\partial r}+\frac{1}{r^2}\frac{\partial^2\psi}{\partial z^2}\frac{\partial^3\psi}{\partial z^2\partial r}-\frac{1}{r^2}\frac{\partial^2\psi}{\partial z^2}\frac{\partial^3\psi}{\partial r^3}-\frac{1}{2r^2}\frac{\partial^2\psi}{\partial r\partial z}\frac{\partial^3\psi}{\partial z^3}-\frac{1}{r^3}(\frac{\partial^2\psi}{\partial z^2})^2]), \tag{28}$$

z-component:

$$-\frac{1}{r}\frac{\partial^2\psi}{\partial r\partial t}+\frac{1}{r}\frac{\partial\psi}{\partial z}(\frac{1}{r^2}\frac{\partial\psi}{\partial r}-\frac{1}{r}\frac{\partial^2\psi}{\partial r^2})+\frac{1}{r^2}\frac{\partial\psi}{\partial r}\frac{\partial^2\psi}{\partial z\partial r}=-\frac{\partial p}{\partial z}+\frac{1}{R_e(1+\lambda_1)}(-\frac{1}{r^3}\frac{\partial\psi}{\partial r}$$
$$+\frac{1}{r^2}\frac{\partial^2\psi}{\partial r^2}-\frac{1}{r}\frac{\partial^3\psi}{\partial r^3}-\frac{1}{r}\frac{\partial^3\psi}{\partial z^2\partial r}+\Lambda_2[-\frac{1}{r^3}\frac{\partial^2\psi}{\partial r\partial t}+\frac{1}{r^2}\frac{\partial^3\psi}{\partial r^2\partial t}-\frac{1}{r}\frac{\partial^4\psi}{\partial z^2\partial r\partial t}-\frac{1}{r}\frac{\partial^4\psi}{\partial r^3\partial t}$$
$$+\frac{1}{r}\frac{\partial\psi}{\partial z}(\frac{2}{r^3}\frac{\partial^2\psi}{\partial z^2}-\frac{1}{r}\frac{\partial^4\psi}{\partial r^2\partial z^2}+\frac{6}{r^4}\frac{\partial\psi}{\partial r}-\frac{6}{r^3}\frac{\partial^2\psi}{\partial r^2}+\frac{3}{r^2}\frac{\partial^3\psi}{\partial r^3}-\frac{1}{r}\frac{\partial^4\psi}{\partial r^4})-\frac{1}{r}\frac{\partial\psi}{\partial r}(-\frac{1}{r^2}\frac{\partial^3\psi}{\partial z^3}$$
$$+\frac{2}{r^2}\frac{\partial^3\psi}{\partial r^2\partial z}-\frac{1}{r}\frac{\partial^4\psi}{\partial r\partial z^3}-\frac{1}{r}\frac{\partial^4\psi}{\partial r^3\partial z})+\frac{1}{r^3}\frac{\partial^2\psi}{\partial r\partial z}\frac{\partial^2\psi}{\partial z^2}+\frac{3}{r^2}\frac{\partial^2\psi}{\partial r\partial z}\frac{\partial^3\psi}{\partial z^2\partial r}+\frac{1}{r^3}\frac{\partial^2\psi}{\partial r^2}\frac{\partial^2\psi}{\partial z\partial r}$$
$$-\frac{1}{r^2}\frac{\partial^3\psi}{\partial r^3}\frac{\partial^2\psi}{\partial z\partial r}-\frac{1}{r^2}\frac{\partial^2\psi}{\partial r^2}\frac{\partial^3\psi}{\partial z^3}-\frac{2}{r^2}\frac{\partial^2\psi}{\partial z^2}\frac{\partial^3\psi}{\partial r^2\partial z}+\frac{1}{r^2}\frac{\partial^2\psi}{\partial r^2}\frac{\partial^3\psi}{\partial r^2\partial z}])+R_N\sigma-R_a\theta+R_M. \tag{29}$$

Eq. of energy becomes:

$$\frac{\partial\theta}{\partial t}+\frac{1}{r}\frac{\partial\psi}{\partial z}\frac{\partial\theta}{\partial r}-\frac{1}{r}\frac{\partial\psi}{\partial r}\frac{\partial\theta}{\partial z}=N_b\left(\frac{\partial\theta}{\partial r}\frac{\partial\sigma}{\partial r}+\frac{\partial\theta}{\partial z}\frac{\partial\sigma}{\partial z}\right)+N_t\left((\frac{\partial\theta}{\partial r})^2+(\frac{\partial\theta}{\partial z})^2\right)$$
$$+\frac{\partial^2\theta}{\partial r^2}+\frac{1}{r}\frac{\partial\theta}{\partial r}+\frac{\partial^2\theta}{\partial z^2}. \tag{30}$$

and the Eq. of nanoparticle volume fraction in the nanofluid becomes:

$$\frac{\tau(C_1-C_0)}{N_b}\left(\frac{\partial\sigma}{\partial t}+\frac{1}{r}\frac{\partial\psi}{\partial z}\frac{\partial\sigma}{\partial r}-\frac{1}{r}\frac{\partial\psi}{\partial r}\frac{\partial\sigma}{\partial z}\right)=\frac{\partial^2\sigma}{\partial r^2}+\frac{1}{r}\frac{\partial\sigma}{\partial r}+\frac{\partial^2\sigma}{\partial z^2}\quad+\frac{N_t}{N_b}\left(\frac{\partial^2\theta}{\partial r^2}+\frac{1}{r}\frac{\partial\theta}{\partial r}+\frac{\partial^2\theta}{\partial z^2}\right). \tag{31}$$

The instantaneous volume flow rate becomes:

$$Q=\int_{r_1}^{r_2}wrdr. \tag{32}$$

The dimensionless boundary conditions are then become:

$$\frac{\partial\psi}{\partial r}=\frac{\gamma^*}{1+\lambda_1}\Big(\frac{\partial^2\psi}{\partial z^2}+\frac{1}{r}\frac{\partial\psi}{\partial r}-\frac{\partial^2\psi}{\partial r^2}+\Lambda_2\Big[\frac{\partial^3\psi}{\partial z^2\partial t}+\frac{1}{r}\frac{\partial^2\psi}{\partial r\partial t}-\frac{\partial^3\psi}{\partial r^2\partial t}+\frac{\partial\psi}{\partial z}\Big(-\frac{1}{r^2}\frac{\partial^2\psi}{\partial z^2}$$

$$+\frac{1}{r}\frac{\partial^3\psi}{\partial r\partial z^2}-\frac{2}{r^3}\frac{\partial\psi}{\partial r}+\frac{2}{r^2}\frac{\partial^2\psi}{\partial r^2}-\frac{1}{r}\frac{\partial^3\psi}{\partial r^3}\Big)-\frac{\partial\psi}{\partial r}\Big(\frac{1}{r}\frac{\partial^3\psi}{\partial z^3}+\frac{1}{r^2}\frac{\partial^2\psi}{\partial r\partial z}-\frac{1}{r}\frac{\partial^3\psi}{\partial r^2}\partial z\Big)\Big]\Big),$$

$$\frac{\partial\psi}{\partial z}=\alpha\varepsilon r\sin\alpha(z-t),\quad \theta+\eta^*\frac{\partial\theta}{\partial r}=1,\quad \sigma+\beta^*\frac{\partial\sigma}{\partial r}=1\quad at\quad r_2=R(z)+h_1, \tag{33}$$

$$\frac{\partial\psi}{\partial z}=0,\quad -\frac{1}{r}\frac{\partial\psi}{\partial r}=V_0^*,\quad \theta=0\quad\text{and}\quad \sigma=0\quad at\quad r=r_1, \tag{34}$$

and

$$h_1=\varepsilon\cos\alpha(z-t). \tag{35}$$

Now, the system of Eqs. (28)-(34) are nonlinear partial differential equations. There is no analytic method to solve them. Therefore, we are forced to consider an approximate solution by using a perturbation technique. This technique is considered in the following section.

3 AN APPROXIMATION SOLUTION

The perturbation technique depends mainly on considering the small parameter as amplitude ratio ε. To solve the nonlinear system of Eqs. (28)-(32) under the appropriate boundary conditions as given by Eq. (33) and (34), we shall assume that any physical quantity, such as ψ, p, θ, σ, Q, the pressure rise Δp and the friction force ΔF may be represented as:

$$\xi=\xi_0+\varepsilon\xi_1+\ldots\ldots, \tag{36}$$

where ξ_0 is the undisturbed quantity and ξ_1 is the first perturbed quantity.

Substituting from Eq. (36) into the system of Eqs. (28)-(34) to collect the terms of like powers of ε. This procedure yields zero and first order systems of partial differential equations according to the corresponding boundary conditions. Through the following subsections, we shall consider these orders:

3.1 THE ZERO-ORDER SYSTEM

Assuming that the radial velocity u is very small in comparison with the axial one w. Also, the variation in the z-direction is smaller than that in the radial one. Therefore, we may assume that $u \ll w$ and $\frac{\partial w}{\partial z} \ll \frac{\partial w}{\partial r}$. Also, it follows that the terms $\frac{\partial u}{\partial r}, \frac{\partial^2 u}{\partial r^2}, \frac{\partial^2 u}{\partial z^2}$ may be ignored [11]. Furthermore, the functions ψ_0, θ_0 and σ_0 may be depended on r only. This case is defined as the initial state (no peristaltic wave). The zero order equations result from the system of Eqs. (28)-(32) may be written as:

r -component:

$$\frac{\partial p_0}{\partial r} = 0, \quad (37)$$

which means that $p_0 = p_0(z)$ only.

z -component:

$$\frac{dp_0}{dz} = \frac{1}{R_e(1+\lambda_1)}\left(\frac{1}{r}\frac{\partial}{\partial r}[r\frac{\partial}{\partial r}(-\frac{1}{r}\frac{\partial \psi_0}{\partial r})]\right) + R_N\sigma_0 - R_a\theta_0 + R_M, \quad (38)$$

$$\frac{1}{r}\frac{\partial}{\partial r}\left(r\frac{\partial \theta_0}{\partial r}\right) + N_b\frac{\partial \theta_o}{\partial r}\frac{\partial \sigma_o}{\partial r} + N_t(\frac{\partial \theta_0}{\partial r})^2 = 0, \quad (39)$$

and

$$\frac{1}{r}\frac{\partial}{\partial r}\left(r\frac{\partial \sigma_0}{\partial r}\right) + \frac{N_t}{N_b}\frac{1}{r}\frac{\partial}{\partial r}\left(r\frac{\partial \theta_0}{\partial r}\right) = 0. \quad (40)$$

The dimensionless volume flow rate become:

$$Q_0 = \int_{r_1}^{R(z)} w_0 r dr, \quad (41)$$

After using Taylor expansion, the boundary conditions (33) and (34) can be written as

$$\frac{\partial \psi_0}{\partial r} = \frac{\gamma^*}{1+\lambda_1}(\frac{1}{r}\frac{\partial \psi_0}{\partial r} - \frac{\partial^2 \psi_0}{\partial r^2}), \quad \frac{\partial \psi_0}{\partial z} = 0, \quad \theta_0 + \eta^*\frac{\partial \theta_0}{\partial r} = 1, \quad \sigma_0 + \beta^*\frac{\partial \sigma_0}{\partial r} = 1 \qquad at \quad r = R(z), \quad (42)$$

$$\frac{\partial \psi}{\partial z_0} = 0, \quad -\frac{1}{r}\frac{\partial \psi_0}{\partial r} = V_0^*, \quad \theta_0 = 0 \quad \text{and} \quad \sigma_0 = 0 \quad at \quad r = r_1. \quad (43)$$

The solutions of Eqs. (38)-(41), in accordance with the boundary conditions (42) and (43), in the case of free pumping or the fluid is stationary, are:

$$\theta_0(r,z) = -\frac{f_2(z)}{N_b f_1(z)} r^{-N_b f_1(z)} + f_3(z), \quad (44)$$

hence, the solution of nanoparticle volume fraction in the nanofluid may be written as

$$\sigma_0(r,z) = \frac{N_t f_2(z)}{N_b^2 f_1(z)} r^{-N_b f_1(z)} + f_1(z)\ln r + f_4(z), \quad (45)$$

$$\psi_0(r,z) = -\frac{f_7(z)}{4 - N_b f_1(z)} r^{4-N_b f_1(z)} - \left(\frac{f_5 G_0(z)}{16} + \frac{4f_6(z) - 5f_8(z)}{16}\right) r^4 - \frac{f_8(z)}{4} r^4 \ln r$$

$$+\left(\frac{(f11(z) - 2f_{13}(z))G_0(z)}{4} + \frac{f_{12}(z) - 2f_{14}(z)}{4}\right) r^2 - \frac{f_{11}(z)G_0(z) + f_{12}(z)}{2} r^2 \ln r, \quad (46)$$

where, $G_0(z)$ is the zero order pressure gradient. Also, the boundary conditions lead to the following implicit transcendental equation in $f_1(z)$:

$$\frac{N_t}{N_b}\left(\frac{\dfrac{(R(z)^{-N_b f_1(z)} - r_1^{-N_b f_1(z)})}{N_b f_1(z)} - \beta^* R(z)^{-N_b f_1(z)-1}}{N_b f_1(z)(r_1^{-N_b f_1(z)} - R(z)^{-N_b f_1(z)}) + \eta^* R(z)^{-N_b f_1(z)-1}}\right) + f_1(z)\ln\frac{R(z)}{r_1} + \beta^*\frac{f_1(z)}{R(z)} \quad = 1. \tag{47}$$

The relation between the pressure gradient and the time mean flow may be written as:

$$G_0(z) = \frac{16}{f_5(R(z)^4 - r_1^4) + 8f_{11}(R(z)^2\ln R(z) - r_1^2\ln r_1) + (2f_{13} - f_{11})(R(z)^2 - r_1^2)}$$

$$\times[\hat{Q} - \frac{1}{16}(4f_6 - 3f_8)(R(z)^4 - r_1^4) - \frac{f_8}{4}$$

$$\times(R(z)^4\ln R(z) - r_1^4\ln r_1) - \frac{f_7}{N_b f_1 + 4}(R(z)^{-N_b f_1+4} - r_1^{-N_b f_1+4}) - \frac{f_{12}}{4}$$

$$\times(2R(z)^2\ln R(z) - 2r_1^2\ln r_1 - R(z)^2 + r_1^2) - f_{14}(R(z) - r_1)], \tag{48}$$

where, $f_i(z)$, $i = 2,6,...,14$ are given in the appendix.

The pressure rise Δp_0, the friction force of inner and outer tubes (ΔF_0^1 and ΔF_0^2), in the tube of length L, in their non -dimensional forms, are given by

$$\Delta p_0 = \int_{-L}^{d} G_0(z)dz$$

$$= \int_{-L}^{-z_0} G_0(z)dz + \int_{-z_0}^{z_0} G_0(z)dz + \int_{z_0}^{d} G_0(z)dz, \tag{49}$$

$$\Delta F_0^1 = \int_{-L}^{d} r_1^2(-G_0(z))dz$$

$$= \int_{-L}^{-z_0} r_1^2(-G_0(z))dz + \int_{-z_0}^{z_0} r_1^2(-G_0(z))dz + \int_{z_0}^{d} r_1^2(-G_0(z))dz, \tag{50}$$

$$\Delta F_0^2 = \int_{-L}^{d} R(z)^2(-G_0(z))dz$$

$$= \int_{-L}^{-z_0} R(z)^2(-G_0(z))dz + \int_{-z_0}^{z_0} R(z)^2(-G_0(z))dz + \int_{z_0}^{d} R(z)^2(-G_0(z))dz. \tag{51}$$

Because of the complexity in evaluating the forgoing integrations, the value of them are computed numerically.

The analytical solutions for the temperature distribution θ_0 and the nanoparticle volume fraction in the nanofluid σ_0 are obtained and expressed in terms of $f_1(z)$, $f_2(z)$, $f_3(z)$ and $f_4(z)$. As $f_2(z)$, $f_3(z)$ and $f_4(z)$ depend on the evaluating of $f_1(z)$, it is noticed from Eq. (35) that $f_1(z)$ is governed by a nonlinear implicit transcendental equation. If this equation is solved for $f_1(z)$, the analytical expression for θ_0 and σ_0 are established. However, it should be observed that obtaining the value of $f_1(z)$ analytically from Eq. (47) in terms of other parameters is very difficult. Therefore, Mathematica software is used to evaluate the numerical solution for this equation. The values for $f_1(z)$ at some cases are presented in tables 1 and 2. These values for $f_1(z)$ play an important role to get several plots.

Table 1. The numerical values of $f_1(z)$ ***at different values of*** N_t ***and*** N_b ***for*** $r_1 = 0.2$, $L = 1$, $\phi = 0.05$, $d = 2$, $\gamma^* = \eta^* = \beta^* = 0.1$, $z_0 = 0.8$ ***and*** $z = 0.4$.

N_b	N_t	f_1
0.8	1	1.3478
	2	1.62155
	3	1.81516
0.9	1	1.23462
	2	1.47487
	3	1.64553
1.0	1	1.14547
	2	1.35861
	3	1.51076

Table 2. The numerical values of $f_1(z)$ ***at different values of*** η^*, β^* ***and*** ϕ ***for*** $r_1 = 0.2$, $L = 1$, $N_t = 2$, $N_b = 0.8$, $d = 2$, $\gamma^* = 0.1$, $z_0 = 0.8$ ***and*** $z = 0.4$.

η^*	β^*	ϕ	f_1
0	0.1	0.05	1.62914
1			1.55115
2			1.46928
0.1	0	0.05	1.67075
	0.4		1.51297
	0.6		1.46191
0.1	0.1	0.05	1.62155
		0	1.56611
		-0.05	1.52212

As a special case of our work, when the maximum height of stenosis, the taper angle, the slip parameters, Brownian motion parameter, thermophoresis parameter, nanoparticles Rayleigh number, thermal Rayleigh number and the ratio of relaxation to retardation times tend to zero in Eqs. (29)

(i.e $r_1 \approx 0, V_0^* = m = h = \lambda_1 = \Lambda_2 = R_N = R_a = R_M = \gamma^* = \eta^* = \beta^* = \phi = N_t = N_b =, f_6 = f_7 = f_8 = f_{11} = f_{12} = f_{14} = 0$, $f_5 = R_e$ and $f_{13} = -\frac{R_e}{4}(\frac{dp_0}{dz})$), we obtain the form $\psi_0(r,z) = \frac{R_e}{8}(\frac{dp_0}{dz})(r^2 - \frac{r^4}{2})$ which is in agreement with the previous work of Fung [30].

3.2 THE FIRST-ORDER SYSTEM

The first order equations that results from the system of Eqs. (28)-(32) may be written as: r-componen

$$\frac{1}{r}\frac{\partial^2\psi_1}{\partial z\partial t}-\frac{1}{r^2}\frac{\partial\psi_0}{\partial r}\frac{\partial^2\psi_1}{\partial z^2}=-\frac{\partial p_1}{\partial r}+\frac{1}{R_e(1+\lambda_1)}(-\frac{1}{r^2}\frac{\partial^2\psi_1}{\partial r\partial z}+\frac{1}{r}\frac{\partial^3\psi_1}{\partial r^2\partial z}+\frac{1}{r}\frac{\partial^3\psi_1}{\partial z^3}$$
$$+\Lambda_2[-\frac{1}{r^2}\frac{\partial^3\psi_1}{\partial r\partial z\partial t}+\frac{1}{r}\frac{\partial^4\psi_1}{\partial r^2\partial z\partial t}+\frac{1}{r}\frac{\partial^4\psi_1}{\partial z^3\partial t}-\frac{1}{r}\frac{\partial\psi_0}{\partial r}(-\frac{3}{r^2}\frac{\partial^3\psi_1}{\partial z^2\partial r}+\frac{1}{r}\frac{\partial^4\psi_1}{\partial r^2\partial z^2}$$
$$+\frac{1}{r}\frac{\partial^4\psi}{\partial z^4}+\frac{4}{r^3}\frac{\partial^2\psi_1}{\partial z^2})+\frac{4}{r^3}\frac{\partial^2\psi_0}{\partial r^2}\frac{\partial^2\psi_1}{\partial z^2}-\frac{2}{r^2}\frac{\partial^2\psi_0}{\partial r^2}\frac{\partial^3\psi_1}{\partial z^2\partial r}-\frac{1}{r^2}\frac{\partial^2\psi_1}{\partial z^2}\frac{\partial^3\psi_0}{\partial r^3}), \tag{52}$$

z-component:

$$-\frac{1}{r}\frac{\partial^2\psi_1}{\partial r\partial t}+\frac{1}{r}\frac{\partial\psi_1}{\partial z}(\frac{1}{r^2}\frac{\partial\psi_0}{\partial r}-\frac{1}{r}\frac{\partial^2\psi_0}{\partial r^2})+\frac{1}{r^2}\frac{\partial\psi_0}{\partial r}\frac{\partial^2\psi_1}{\partial z\partial r}=-\frac{\partial p_1}{\partial z}+\frac{1}{R_e(1+\lambda_1)}(-\frac{1}{r^3}\frac{\partial\psi_1}{\partial r}$$
$$+\frac{1}{r^2}\frac{\partial^2\psi_1}{\partial r^2}-\frac{1}{r}\frac{\partial^3\psi_1}{\partial r^3}-\frac{1}{r}\frac{\partial^3\psi_1}{\partial z^2\partial r}+\Lambda_2[-\frac{1}{r^3}\frac{\partial^2\psi_1}{\partial r\partial t}+\frac{1}{r^2}\frac{\partial^3\psi}{\partial r^2\partial t}-\frac{1}{r}\frac{\partial^4\psi}{\partial z^2\partial r\partial t}-\frac{1}{r}\frac{\partial^4\psi_1}{\partial r^3\partial t}$$
$$+\frac{1}{r}\frac{\partial\psi_1}{\partial z}(\frac{6}{r^4}\frac{\partial\psi_0}{\partial r}-\frac{6}{r^3}\frac{\partial^2\psi_0}{\partial r^2}+\frac{3}{r^2}\frac{\partial^3\psi_0}{\partial r^3}-\frac{1}{r}\frac{\partial^4\psi_0}{\partial r^4})-\frac{1}{r}\frac{\partial\psi_0}{\partial r}(-\frac{1}{r^2}\frac{\partial^3\psi_1}{\partial z^3}+\frac{2}{r^2}\frac{\partial^3\psi_1}{\partial r^2\partial z}$$
$$-\frac{1}{r}\frac{\partial^4\psi_1}{\partial r\partial z^3}-\frac{1}{r}\frac{\partial^4\psi_1}{\partial r^3\partial z})+\frac{1}{r^3}\frac{\partial^2\psi_0}{\partial r^2}\frac{\partial^2\psi_1}{\partial z\partial r}-\frac{1}{r^2}\frac{\partial^3\psi_0}{\partial r^3}\frac{\partial^2\psi_1}{\partial z\partial r}-\frac{1}{r^2}\frac{\partial^2\psi_0}{\partial r^2}\frac{\partial^3\psi_1}{\partial z^3}$$
$$+\frac{1}{r^2}\frac{\partial^2\psi_0}{\partial r^2}\frac{\partial^3\psi_1}{\partial r^2\partial z}])+R_N\sigma_1-R_a\theta_1. \tag{53}$$

Eq. of energy becomes:

$$\frac{\partial\theta_1}{\partial t}+\frac{1}{r}\frac{\partial\psi_1}{\partial z}\frac{\partial\theta_0}{\partial r}-\frac{1}{r}\frac{\partial\psi_0}{\partial r}\frac{\partial\theta_1}{\partial z}=N_b\left(\frac{\partial\theta_1}{\partial r}\frac{\partial\sigma_0}{\partial r}+\frac{\partial\theta_0}{\partial r}\frac{\partial\sigma_1}{\partial r}\right)+2N_t\frac{\partial\theta_0}{\partial r}\frac{\partial\theta_1}{\partial r}$$
$$+\frac{\partial^2\theta_1}{\partial r^2}+\frac{1}{r}\frac{\partial\theta_1}{\partial r}+\frac{\partial^2\theta_1}{\partial z^2}, \tag{54}$$

and the Eq. of nanoparticle volume fraction in the nanofluid becomes:

$$\frac{\tau(C_1-C_0)}{N_b}\left(\frac{\partial\sigma_1}{\partial t}+\frac{1}{r}\frac{\partial\psi_1}{\partial z}\frac{\partial\sigma_0}{\partial r}-\frac{1}{r}\frac{\partial\psi_0}{\partial r}\frac{\partial\sigma_1}{\partial z}\right)=\frac{\partial^2\sigma_1}{\partial r^2}+\frac{1}{r}\frac{\partial\sigma_1}{\partial r}+\frac{\partial^2\sigma_1}{\partial z^2}$$
$$+\frac{N_t}{N_b}\left(\frac{\partial^2\theta_1}{\partial r^2}+\frac{1}{r}\frac{\partial\theta_1}{\partial r}+\frac{\partial^2\theta_1}{\partial z^2}\right). \tag{55}$$

After using Taylor expansion the boundary conditions can be written as

$$\frac{\partial\psi_1}{\partial r}+\cos\alpha(z-t)\frac{\partial^2\psi_1}{\partial r^2}=\frac{\gamma^*}{1+\lambda_1}(\frac{\partial^2\psi_1}{\partial z^2}+\frac{1}{r}\frac{\partial\psi_1}{\partial r}-\frac{\partial^2\psi_1}{\partial r^2}+\cos\alpha(z-t)(\frac{1}{r}\frac{\partial^2\psi_1}{\partial r^2}-\frac{\partial^3\psi_1}{\partial r^3})$$
$$+\Lambda_2[\frac{\partial^3\psi_1}{\partial z^2\partial t}+\frac{1}{r}\frac{\partial^2\psi_1}{\partial r\partial t}-\frac{\partial^3\psi_1}{\partial r^2\partial t}+\frac{\partial\psi_1}{\partial z}(-\frac{2}{r^3}\frac{\partial\psi_0}{\partial r}+\frac{2}{r^2}\frac{\partial^2\psi_0}{\partial r^2}-\frac{1}{r}\frac{\partial^3\psi_0}{\partial r^3})-\frac{\partial\psi_0}{\partial r}(\frac{1}{r}\frac{\partial^3\psi_1}{\partial z^3}$$

$$+\frac{1}{r^2}\frac{\partial^2\psi_1}{\partial r\partial z}-\frac{1}{r}\frac{\partial^3\psi_1}{\partial r^2}\partial z)]),\quad \frac{\partial\psi_1}{\partial z}=\alpha R(z)\sin\alpha(z-t),$$

$$\theta_1+\eta^*\frac{\partial\theta_1}{\partial r}+\cos\alpha(z-t)(\theta_0+\eta^*\frac{\partial\theta_0}{\partial r})=0,\quad \sigma_1+\beta^*\frac{\partial\sigma_1}{\partial r}+\cos\alpha(z-t)(\sigma_0+\beta^*\frac{\partial\sigma_0}{\partial r})=0$$

$$at\quad r_2=R(z), \tag{56}$$

$$\frac{\partial\psi_1}{\partial z}=0,\quad \frac{\partial\psi_1}{\partial r}=0,\quad \theta_1=0\quad \text{and}\quad \sigma_1=0\quad at\quad r=r_1. \tag{57}$$

The solutions for ψ_1, θ_1 and σ_1 may be considered along the normal mode analysis [30]. Therefore, the various physical quantities may be represented as:

$$\psi_1=A_1(r)\exp[i\alpha(z-t)]+c.c.,$$
$$\theta_1=J_1(r)\exp[i\alpha(z-t)]+c.c.,$$
$$\sigma_1=B_1(r)\exp[i\alpha(z-t)]+c.c., \tag{58}$$

where the c.c. denotes to the complex conjugate of the preceding term.

Substituting from (58) in (52)-(57), we get the following system of ordinary differential equations:

$$i\alpha A_1\left(\frac{\alpha^2}{r}+\frac{2f_{11}G_0}{r^3}-f_7f_1N_b(f_1N_b-2)r^{-f_1N_b-1}+\frac{4f_8}{r}+\frac{2f_{12}}{r^3}\right)-i\alpha\frac{d^2A_1}{dr^2}+\frac{i\alpha}{r^2}\frac{dA_1}{dr}$$
$$+\left((\frac{f_5r}{4}+\frac{f_{11}\ln r}{r}+\frac{f_{13}}{r})G_0+(f_6-f_8)r+f_7r^{-f_1N_b+1}+f_8r\ln r+\frac{f_{12}\ln r}{r}+\frac{f_{14}}{r}\right)$$
$$\times\left(-i\alpha^3A_1+i\alpha\frac{d^2A_1}{dr^2}-\frac{i\alpha}{r}\frac{dA_1}{dr}\right)=\frac{1}{R_e(1+\lambda_1)}(\frac{2\alpha^2}{r^2}\frac{dA_1}{dr}-\frac{2\alpha^2}{r}\frac{dA_1}{dr}+\frac{1}{r}\frac{d^4A_1}{dr^4}$$
$$-\frac{3}{r^4}\frac{dA_1}{dr}+\frac{3}{r^3}\frac{d^2A_1}{dr^2}-\frac{2}{r^2}\frac{d^3A_1}{dr^3}+\Lambda_2[(-\frac{2i\alpha^3}{r^2}+\frac{3i\alpha}{r^4})\frac{dA_1}{dr}+(\frac{2i\alpha^3}{r}-\frac{3i\alpha}{r^3})\frac{d^2A_1}{dr^2}-\frac{i\alpha}{r}\frac{d^4A_1}{dr^4}$$
$$+i\alpha A_1\left(\frac{9f_{11}G_0}{r^5}-f_7N_bf_1(N_b^3f_1^3-N_b^2f_1^2-4N_bf_1+4)r^{-N_bf_1-3}+\frac{4f_8}{r^3}+\frac{8f_{12}}{r^5}\right)$$
$$+\frac{2i\alpha}{r^2}\frac{d^3A_1}{dr^3}-i\alpha\frac{dA_1}{dr}((-\frac{3f_5}{r^2}+\frac{3f_{11}\ln r+f_{11}+8f_{13}}{r^4})G_0-\frac{12(f_6-f_8)}{r^2}$$
$$-f_7r^{-N_bf_1-2}(12+17N_bf_1-6N_b^2f_1^2+2N_b^3f_1^3)-\frac{f_8}{r^2}(12\ln r+1)+\frac{3f_{12}\ln r+3f_{14}+1}{r^4})$$
$$+\left((\frac{f_5r^3}{4}+f_{11}r\ln r+f_{13}r)G_0+(f_6-f_8)r^3+f_7r^{-N_bf_1+3}+f_8r^3\ln r+f_{12}r\ln r+f_{14}r\right)$$
$$\times\left((-\frac{i\alpha^3}{r^3}+\frac{i\alpha^5}{r^2})A_1+\frac{4i\alpha^3}{r^3}\frac{dA_1}{dr}+(\frac{6i\alpha}{r^4}-\frac{2i\alpha^3}{r^2})\frac{d^2A_1}{dr^2}-\frac{4i\alpha}{r^3}\frac{d^3A_1}{dr^3}+\frac{i\alpha}{r^2}\frac{d^4A_1}{dr^4}\right)$$
$$((\frac{3f_5r^2}{4}+f_{11}(\ln r+1)+f_{13})G_0+3(f_6-f_8)r^2+f_7(3-N_bf_1)r^{-N_bf_1+2}+f_{12}(\ln r+1)$$

$$+ f_8 r^2(3\ln r + 1) + f_{14}\left(-\frac{i\alpha^3}{r^3} A_1 + \frac{2i\alpha^3}{r^2}\frac{dA_1}{dr} + \frac{3i\alpha}{r^3}\frac{d^2A_1}{dr^2} - \frac{2i\alpha}{r^2}\frac{d^3A_1}{dr^3} \right)])$$

$$- R_N \frac{dB_1}{dr} + R_a \frac{dJ_1}{dr}, \tag{59}$$

$$i\alpha J_1(-1 + (\frac{f_5 r^2}{4} + f_{11}\ln r + f_{13})G_0 + (f_6 - f_8)r^2 + f_7 r^{-f_1 N_b + 2} + f_8 r^2 \ln r + f_{12}\ln r + f_{14}))$$

$$+ i\alpha f_2 A_1 r^{-N_b f_1 - 2} = \frac{d^2 J_1}{dr^2} + \left(N_t f_2 r^{-N_b f_1 - 1} + \frac{N_b f_1 + 1}{r} \right)\frac{dJ_1}{dr} - \alpha^2 J_1$$

$$+ N_b f_2 r^{-N_b f_1 - 1}\frac{dB_1}{dr}, \tag{60}$$

$$\frac{i\alpha\tau(C_1 - C_0)}{N_b}(A_1(\frac{-N_t f_2}{N_b} r^{-N_b f_1 - 2} + \frac{f_1}{r^2}) + B_1(-1 + (\frac{f_5 r^2}{4} + f_{11}\ln r + f_{13})G_0 + (f_6 - f_8)r^2$$

$$+ f_7 r^{-f_1 N_b + 2} + f_8 r^2 \ln r + f_{12}\ln r + f_{14})) = \frac{d}{dr}(r\frac{dB_1}{dr}) + \frac{N_t}{N_b}(\frac{d}{dr}(r\frac{dJ_1}{dr}))$$

$$- \alpha^2(B_1 + \frac{N_t}{N_b} J_1), \tag{61}$$

with the appropriate boundary conditions:

$$\frac{dA_1}{dr} - \frac{G_0}{2}(\frac{3f_5 R^2}{4} + f_{11}(1 + \ln R) + f_{13}) - \frac{3}{2}(f_6 - f_8)R^2 - \frac{f_7}{2}(3 - N_b f_1)R^{2 - N_b f_1}$$

$$- \frac{f_8}{2} R^2(1 + 2\ln R) - \frac{f_{12}}{2}(1 + \ln R) - \frac{f_{14}}{2} = \frac{\gamma^*}{1 + \lambda_1}(-\alpha^2 A_1 + \frac{1}{R}\frac{dA_1}{dr} - \frac{d^2 A_1}{dr^2}$$

$$+ \frac{G_0}{2}(\frac{3f_5 R}{4} - \frac{f_{11}}{R}\ln R - \frac{f_{13}}{R}) + \frac{3}{2}(f_6 - f_8)R + \frac{f_7}{2}(3 - 4N_b f_1 + N_b^2 f_1^2)R^{-1 - N_b f_1}$$

$$+ \frac{f_8}{2} R(-4 + 3\ln R) - \frac{f_{12}}{2}\frac{\ln R}{R} - \frac{f_{14}}{2R} + \Lambda_2[-\frac{i\alpha}{R}\frac{dA_1}{dr} + i\alpha\frac{d^2 A_1}{dr^2} + i\alpha A_1(\alpha^2$$

$$+ G_0(\frac{f_5}{2} - \frac{f_{11}}{R^2}) + 2(f_6 - f_8) + f_7(2 - 3N_b f_1 + N_b^2 f_1^2)R^{-N_b f_1} + f_8(3 + 2\ln R))$$

$$+ (G_0(\frac{f_5 R^3}{4} + \frac{f_{11}}{R}\ln R - f_{13}R) + (f_6 - f_8)R^3 + f_7 R^{3 - N_b f_1} + f_8 R^3 \ln R \quad 18pt$$

$$+ f_{12}\ln R + f_{14} r)(\frac{i\alpha}{R^2}\frac{dA_1}{dr} - \frac{i\alpha}{R}\frac{d^2 A_1}{dr^2} - \frac{i\alpha^3}{R} A_1)]), \quad 18pt A_1 = -\frac{R}{2},$$

$$B_1 + \beta^*\frac{dB_1}{dr} = \frac{1}{2}(\beta^*(\frac{f_1}{R^2} - \frac{N_t}{N_b}(N_b f_1 + 1)f_2 R^{-N_b f_1 - 2}) + \frac{N_t}{N_b} f_2 R^{-N_b f_1 - 1} - \frac{f_1}{R}),$$

$$J_1+\eta^*\frac{dJ_1}{dr}=\frac{f_2R^{-N_bf_1-1}}{2}\left(\frac{\eta^*(N_bf_1+1)}{R}-1\right)\quad at\quad r=R(z), \tag{62}$$

$$A_1=\frac{dA_1}{dr}=J_1=B_1=0\quad at\quad r=r_1. \tag{63}$$

Eqs. (59)-(61) represents a system of nonlinear partial differential equations. Therefore, it is impossible to find their solutions in a closed form for arbitrary values of the given parameters. Even for non-Newtonian fluids [6], the required solutions are given by a perturbation technique. Following Jaffrin [32], the long wavelength approximation is considered. This requires that the wave number α is small. Therefore, the flow quantities, such as $A_1(r)$, $J_1(r)$ and $B_1(r)$, may be expanded in a power series of the small parameter α as follows:

$$\chi_1(r)=\chi_{10}(r)+\alpha\chi_{11}(r)+..... \tag{64}$$

Substituting from Eq. (64) into Eqs. (59)-(61) and collecting the terms of like powers of α. Another zero and first order according to the parameter α are considered. These orders may be solved analytically in the following subsections.

3.2.1 THE ZERO-ORDER SYSTEM OF α

The zero-order equations that results from (59)-(61) can be written as

$$\frac{d}{dr}\left(\frac{1}{r}\frac{d}{dr}\right)\left(r\frac{d}{dr}\left(\frac{1}{r}\frac{d}{dr}\right)\right)A_{10}=R_e(1+\lambda_1)\left(R_N\frac{dB_{10}}{dr}-R_a\frac{dJ_{10}}{dr}\right), \tag{65}$$

$$\frac{d^2J_{10}}{dr^2}+\left(N_tf_2r^{-N_bf_1-1}+\frac{N_bf_1+1}{r}\right)\frac{dJ_{10}}{dr}+N_bf_2r^{-N_bf_1-1}\frac{dB_{10}}{dr}=0, \tag{66}$$

$$\frac{d}{dr}\left(r\frac{dB_{10}}{dr}\right)+\frac{N_t}{N_b}\left(\frac{d}{dr}\left(r\frac{dJ_{10}}{dr}\right)\right)=0, \tag{67}$$

with the appropriate boundary conditions:

$$\frac{dA_{10}}{dr}-\frac{G_0}{2}\left(\frac{3f_5R^2}{4}+f_{11}(1+\ln R)+f_{13}\right)-\frac{3}{2}(f_6-f_8)R^2-\frac{f_7}{2}(3-N_bf_1)R^{2-N_bf_1}$$

$$-\frac{f_8}{2}R^2(1+2\ln R)-\frac{f_{12}}{2}(1+\ln R)-\frac{f_{14}}{2}=\frac{\gamma^*}{1+\lambda_1}\left(\frac{1}{R}\frac{dA_{10}}{dr}-\frac{d^2A_{10}}{dr^2}\right.$$

$$+\frac{G_0}{2}\left(\frac{3f_5R}{4}-\frac{f_{11}}{R}\ln R-\frac{f_{13}}{R}\right)+\frac{3}{2}(f_6-f_8)R+\frac{f_7}{2}(3-4N_bf_1+N_b^2f_1^2)R^{-1-N_bf_1}$$

$$\left.+\frac{f_8}{2}R(-4+3\ln R)-\frac{f_{12}}{2}\frac{\ln R}{R}-\frac{f_{14}}{2R}\right),\quad A_{10}=-\frac{R}{2},$$

$$B_{10}+\beta^*\frac{dB_{10}}{dr}=\frac{1}{2}\left(\beta^*\left(\frac{f_1}{R^2}-\frac{N_t}{N_b}(N_bf_1+1)f_2R^{-N_bf_1-2}\right)+\frac{N_t}{N_b}f_2R^{-N_bf_1-1}-\frac{f_1}{R}\right),$$

$$J_{10}+\eta^*\frac{dJ_{10}}{dr}=\frac{f_2R^{-N_bf_1-1}}{2}\left(\frac{\eta^*(N_bf_1+1)}{R}-1\right)\quad at\quad r=R(z), \tag{68}$$

$$A_{10} = \frac{dA_{10}}{dr} = J_{10} = B_{10} = 0 \quad at \quad r = r_1. \tag{69}$$

The solutions of zero-order system of α take the following forms:

$$J_{10} = f_{16}(z) + f_{17}(z) r^{-N_b f_1} + \frac{f_2(z) f_{15}(Z)}{f1(Z)} r^{-N_b f_1} \ln r, \tag{70}$$

$$B_{10} = f_{18}(z) - \frac{f_1(z) f_{17}(z) N_t}{N_b f_1} r^{-N_b f_1} - \frac{f_2(z) f_{15}(Z) N_t}{N_b f1(Z)} r^{-N_b f_1} \ln r + f_{15}(z) \ln r, \tag{71}$$

$$A_{10} = f_{27}(z) r^{4-N_b f_1} + f_{26}(z) r^4 + f_{28}(z) r^2 + f_{29}(z) r^4 \ln r + f_{30}(z) r^{4-N_b f_1} \ln r + \frac{f_{23}(z)}{2} r^2 \ln r + f_{24}(z) \ln r + f_{25}(z), \tag{72}$$

where the constants $f_i(z)$, i =15,16,....,30, are given in the appendix.

3.2.2 THE FIRST-ORDER SYSTEM OF α

The first-order equations that results from (59)-(61) can be written in the following ordinary differential equations

$$iA_{10}\left(\frac{2f_{11}G_0}{r^3} - f_7 f_1 N_b (f_1 N_b - 2) r^{-f_1 N_b - 1} + \frac{4f_8}{r} + \frac{2f_{12}}{r^3}\right) - i\frac{d^2 A_{10}}{dr^2} + \frac{i}{r^2}\frac{dA_{10}}{dr}$$

$$+\left((\frac{f_5 r}{4} + \frac{f_{11}\ln r}{r} + \frac{f_{13}}{r})G_0 + (f_6 - f_8) r + f_7 r^{-f_1 N_b + 1} + f_8 r \ln r + \frac{f_{12}\ln r}{r} + \frac{f_{14}}{r}\right)$$

$$\times\left(i\frac{d^2 A_{10}}{dr^2} - \frac{i}{r}\frac{dA_{10}}{dr}\right) = \frac{1}{R_e(1+\lambda_1)}(\frac{1}{r}\frac{d^4 A_{11}}{dr^4} - \frac{3}{r^4}\frac{dA_{11}}{dr} + \frac{3}{r^3}\frac{d^2 A_{11}}{dr^2} - \frac{2}{r^2}\frac{d^3 A_{11}}{dr^3}$$

$$+\Lambda_2[\frac{3i}{r^4}\frac{dA_{10}}{dr} - \frac{3i}{r^3}\frac{d^2 A_{10}}{dr^2} - \frac{i}{r}\frac{d^4 A_{10}}{dr^4} + \frac{2i}{r^2}\frac{d^3 A_{10}}{dr^3} - i\frac{dA_{10}}{dr}((-\frac{3f_5}{r^2} + \frac{3f_{11}\ln r + f_{11} + 8f_{13}}{r^4})G_0$$

$$-\frac{12(f_6 - f_8)}{r^2} - f_7 r^{-N_b f_1 - 2}(12 + 17 N_b f_1 - 6N_b^2 f_1^2 + 2N_b^3 f_1^3) - \frac{f_8}{r^2}(12\ln r + 1)$$

$$+\frac{3f_{12}\ln r + 3f_{14} + 1}{r^4}) + \left(\frac{6i}{r^4}\frac{d^2 A_{10}}{dr^2} - \frac{4i}{r^3}\frac{d^3 A_{10}}{dr^3} + \frac{i}{r^2}\frac{d^4 A_{10}}{dr^4}\right)$$

$$\times\left((\frac{f_5 r^3}{4} + f_{11} r \ln r + f_{13} r)G_0 + (f_6 - f_8) r^3 + f_7 r^{-N_b f_1 + 3} + f_8 r^3 \ln r + f_{12} r \ln r + f_{14} r\right)$$

$$+iA_{10}\left(\frac{9f_{11}G_0}{r^5} - f_7 N_b f_1 (N_b^3 f_1^3 - N_b^2 f_1^2 - 4N_b f_1 + 4) r^{-N_b f_1 - 3} + \frac{4f_8}{r^3} + \frac{8f_{12}}{r^5}\right)$$

$$+((\frac{3f_5 r^2}{4} + f_{11}(\ln r + 1) + f_{13})G_0 + 3(f_6 - f_8) r^2 + f_7(3 - N_b f_1) r^{-N_b f_1 + 2} + f_{12}(\ln r + 1)$$

$$+f_8 r^2 (3\ln r + 1) + f_{14})\left(\frac{3i}{r^3}\frac{d^2 A_{10}}{dr^2} - \frac{2i}{r^2}\frac{d^3 A_{10}}{dr^3}\right]) - R_N \frac{dB_{10}}{dr} + R_a \frac{dJ_{10}}{dr}, \tag{73}$$

$$iJ_{10}\left(1+(\frac{f_5 r^2}{4}+f_{11}\ln r+f_{13})G_0+(f_6-f_8)r^2+f_7 r^{-f_1 N_b+2}+f_8 r^2\ln r+f_{12}\ln r+f_{14}\right)$$

$$+if_2 A_{10} r^{-N_b f_1-2}=\frac{d^2 J_{11}}{dr^2}+\left(N_t f_2 r^{-N_b f_1-1}+\frac{N_b f_1+1}{r}\right)\frac{dJ_{11}}{dr}+N_b f_2 r^{-N_b f_1-1}\frac{dB_{11}}{dr}, \quad (74)$$

$$\frac{i\tau(C_1-C_0)}{N_b}(A_{10}(\frac{-N_t f_2}{N_b}r^{-N_b f_1-2}+\frac{f_1}{r^2})+B_{10}(-1+(\frac{f_5 r^2}{4}+f_{11}\ln r+f_{13})G_0+(f_6-f_8)r^2$$

$$+f_7 r^{-f_1 N_b+2}+f_8 r^2\ln r+f_{12}\ln r+f_{14}))=\frac{d}{dr}(r\frac{dB_{11}}{dr})+\frac{N_t}{N_b}(\frac{d}{dr}(r\frac{dJ_{11}}{dr})), \quad (75)$$

with the appropriate boundary conditions:

$$\frac{dA_{11}}{dr}=\frac{\gamma^*}{1+\lambda_1}(\frac{1}{R}\frac{dA_{11}}{dr}-\frac{d^2A_{11}}{dr^2}+\Lambda_2[-\frac{i}{R}\frac{dA_{10}}{dr}+i\frac{d^2A_{10}}{dr^2}+iA_{10}(G_0(\frac{f_5}{2}-\frac{f_{11}}{R^2})$$

$$+2(f_6-f_8)+f_7(2-3N_b f_1+N_b^2 f_1^2)R^{-N_b f_1}+f_8(3+2\ln R))$$

$$+(G_0(\frac{f_5 R^3}{4}+\frac{f_{11}}{R}\ln R-f_{13}R)+(f_6-f_8)R^3+f_7 R^{3-N_b f_1}+f_8 R^3\ln R$$

$$+f_{12}\ln R+f_{14}r)(\frac{i}{R^2}\frac{dA_{10}}{dr}-\frac{i}{R}\frac{d^2A_{10}}{dr^2})]), \quad A_{11}=0,$$

$$B_{11}+\beta^*\frac{dB_{11}}{dr}=0, \quad J_{11}+\eta^*\frac{dJ_{11}}{dr}=0 \quad at \quad r=R(z), \quad (76)$$

$$A_{11}=\frac{dA_{11}}{dr}=J_{11}=B_{11}=0 \quad at \quad r=r_1. \quad (77)$$

The solutions of first-order system of α take the following forms:

$$J_{11}=i(f_{150}r^2+f_{151}r^4+f_{152}r^{2-N_b f_1}+f_{154}r^{4-N_b f_1}+f_{162}r^{2-2N_b f_1}$$

$$+f_{163}r^{4-3N_b f_1}+f_{165}r^{-2N_b f_1}+f_{168}r^{-2-2N_b f_1}+f_{131}r^{4-2N_b f_1}$$

$$+(\frac{f_{192}-f_{194}}{f_{193}-f_{191}}(f_{137}-\frac{f_2}{N_b f_1^2})+f_{136}+f_{104})r^{-N_b f_1}+\frac{(f_{192}-f_{194})(f_{160}-f_{161})}{f_{193}-f_{191}}$$

$$+f_{136}-f_{111}+[(\frac{f_{192}-f_{194}}{f_{193}-f_{191}}N_b f_2+f_{156})r^{-N_b f_1}+f_{157}r^2+f_{158}r^4$$

$$+f_{153}r^{2-N_b f_1}+f_{155}r^{4-N_b f_1}+f_{106}r^{4-2N_b f_1}+f_{170}r^{2-2N_b f_1}+f_{164}r^{4-3N_b f_1}$$

$$+f_{166}r^{-2N_b f_1}]\ln r+[f_{159}r^{2-N_b f_1}+f_{171}r^{4-N_b f_1}$$

$$+f_{167}r^{-N_b f_1}+f_{169}r^{2-2N_b f_1}+f_{172}r^{4-2N_b f_1}](\ln r)^2+f_{134}r^{-N_b f_1}(\ln r)^3), \quad (78)$$

$$B_{11}=i(\frac{f_{50}}{2r^2}+f_{178}r^2+f_{179}r^4+f_{180}r^{2-N_b f_1}+f_{182}r^{4-N_b f_1}+f_{184}r^{4-2N_b f_1}$$

$$-\frac{N_t}{N_b}(f_{162}r^{2-2N_bf_1}+f_{163}r^{4-3N_bf_1}+f_{165}r^{-2N_bf_1}+f_{168}r^{-2-2N_bf_1})$$

$$+(\frac{f_{192}-f_{194}}{f_{193}-f_{191}}f_{174}+f_{177})r^{-N_bf_1}+\frac{(f_{192}-f_{194})f_{173}+f_{194}f_{191}-f_{192}f_{193}}{f_{193}-f_{191}}$$

$$+f_{176}+[\frac{f_{192}-f_{194}}{f_{193}-f_{191}}+(\frac{f_{192}-f_{194}}{f_{193}-f_{191}}f_{175}+f_{186})r^{-N_bf_1}+f_{187}r^2+f_{188}r^4$$

$$+f_{181}r^{2-N_bf_1}+f_{183}r^{4-N_bf_1}+f_{185}r^{4-2N_bf_1}-\frac{N_t}{N_b}(f_{170}r^{2-2N_bf_1}+f_{164}r^{4-3N_bf_1}$$

$$+f_{166}r^{-2N_bf_1})]\ln r+[f_{189}r^{2-N_bf_1}+f_{190}r^{4-N_bf_1}+f_{61}+\frac{f_{53}}{4}r^2+\frac{f_{55}}{8}r^4$$

$$-\frac{N_t}{N_b}(f_{167}r^{-N_bf_1}+f_{169}r^{2-2N_bf_1}+f_{172}r^{4-2N_bf_1})](\ln r)^2+[-\frac{N_t}{N_b}f_{134}r^{-N_bf_1}$$

$$18pt+\frac{f_{52}}{6}](\ln r)^3), \tag{79}$$

$$A_{11}=i(f_{347}r^8+f_{345}r^6+(f_{349}+\frac{f_{389}}{16})r^4+\frac{1}{2}(f_{391}-\frac{f_{390}}{4})r^2+f_{392}+f_{352}r^{8-N_bf_1}$$

$$+f_{353}r^{8-2N_bf_1}+f_{351}r^{6-N_bf_1}+f_{355}r^{6-2N_bf_1}+f_{354}r^{4-N_bf_1}+f_{356}r^{2-N_bf_1}+f_{357}r^{8-3N_bf_1}$$

$$+f_{358}r^{4-2N_bf_1}+f_{359}r^{2-2N_bf_1}+f_{360}r^{9-2N_bf_1}+f_{361}r^{8-4N_bf_1}+[f_{346}r^8+f_{344}r^6+f_{348}r^4$$

$$+\frac{f_{390}}{2}r^2+f_{316}+f_{370}r^{8-N_bf_1}+f_{365}r^{8-2N_bf_1}+f_{362}r^{6-N_bf_1}+f_{367}r^{6-2N_bf_1}+f_{363}r^{4-N_bf_1}$$

$$+f_{356}r^{2-N_bf_1}+f_{368}r^{8-3N_bf_1}+f_{369}r^{4-2N_bf_1}+f_{364}r^{8-4N_bf_1}]\ln r+[\frac{f_{216}}{1152}r^8+\frac{f_{124}}{192}r^6$$

$$+f_{350}r^4+\frac{f_{249}}{8}+f_{373}r^{8-N_bf_1}+f_{375}r^{8-2N_bf_1}+f_{371}r^{6-N_bf_1}+f_{372}r^{6-2N_bf_1}$$

$$+f_{374}r^{4-N_bf_1}](\ln r)^2+[\frac{f_{224}}{48}r^4+\frac{f_{241}}{6}+f_{376}r^{4-N_bf_1}](\ln r)^3+\frac{f_{242}}{24}(\ln r)^4+\frac{f_{252}}{60}(\ln r)^5, \tag{80}$$

where the constants $f_i(z)$, i =31,32,....,392, are obtained during the calculations and are given in the appendix.

4 DISCUSSION OF THE RESULTS

In what follows, numerical calculations will be made. It is convenient to classify these calculations into two categories, as follows:

4.1 PUMPING CHARACTERISTICS

In order to identify the quantitative effects of various parameters on the obtained distributions of the axial velocity w, temperature θ, nanoparticle volume fraction in the nanofluid σ, pressure rise ΔP and friction force of the outer tube ΔF_2, the mathematical software (Mathematica) is used. Some important results are graphically displayed in Figures 2-8 as follows.

Figure 2-A describes the variation of axial velocity w versus (vs) z -axis for different values of the nanoparticles Grashof number R_N. It is observed that, at the domain ($-0.4 \le z \le 0.6$), the axial velocity increases with the increase of R_N. Therefore, it is depicted that nanofluid, with high concentration of nanoparticles possesses, cause higher values of the velocity. So, higher nanoparticles volume fraction provides more resistance to the flow. Meanwhile, at the complementary of this domain, the axial velocity decreases with the increase of R_N. Figure 2-B indicates the variation of axial velocity $w(z)$ for different values of the local temperature Grashof number R_a. It is showed that R_a has the same effects as that of R_N on the axial velocity profile. Figure 2-C shows the variation of axial velocity $w(z)$ for different values of the maximum height of stenosis h. It is observed that when the domain of z becomes ($-0.8 \le z \le 0.8$), the axial velocity decreases with the increase of h. Meanwhile, at the complementary of this domain, the curves of these velocities are coincide to each others. It is also found that, in case of no-stenosis ($h = 0$), the values of the axial velocity is greater than that in case of stenosis. Therefore, for the diseases of blood clot, the existence of the clots at the artery straitens the blood flow and leads to a harmful effects for the body organs [9]. Figure 2-D indicates the variation of axial velocity $w(z)$ for different values of the velocity slip parameter γ^*. It is observed that the axial velocity decreases with the increase of γ^*. It is also found that, in case of no-slip condition ($\gamma^* = 0$), the value of the axial velocity is higher than that in case of slip condition.

Figure 3-A indicates the variation of axial velocity w vs the radial distance r for different values of the taper angle ϕ. The importance of the effect of vessel tapering with the shape of stenosis deserves special attention. Also, the tapering has a significant aspect arterial system [11]. Therefore, we are interested in studying the flow through a tapered tube with stenosis. It is observed that, at the domain ($0.2 \le r \le 0.8$), in case of the diverging tapered artery $\phi = 0.05 (> 0)$, the values of the axial velocity are smaller than those in case of the non tapered artery $\phi = 0$ and the convergent tapered one $\phi = -0.05 (< 0)$. However, at the complementary of this domain, the inverse occurs. Figure 3-B shows the variation of axial velocity $w(r)$ for different values of the ratio of relaxation time to retardation one λ_1. It indicates that, at the domain ($0.2 \le r \le 0.8$), the axial velocity increases with the increase of λ_1. It is also found that, in case of Newtonian fluid ($\lambda_1 = 0$), the value of the axial velocity is lower than that in case of non-Newtonian fluid. Meanwhile, at the complementary of this domain, the axial velocity decreases with the increase of λ_1. It is also noted that, in case of Newtonian fluid ($\lambda_1 = 0$), the value of the axial velocity is greater than that in case of non-Newtonian fluid. Figure 3-C indicates the variation of axial velocity $w(r)$ for different values of the flow rate Q. It is observed that, at the domain ($0.2 \le r \le 0.8$), the axial velocity decreases by the increasing of Q. However, the inverse occurs at the at the complementary of this domain. Figure 3-D indicates the variation of axial velocity $w(z)$ for different values of the Reynolds number R_e. It is observed that, the axial velocity increases with the increase of R_e. Through this figure, the numerical calculations depict that as the Reynolds number increase, both of viscosity and flow resistance are decreased, the axial velocity is also increased.

The special case of ignoring the parameters $\phi = 0$ (no-tapered), $h = 0$ (no-stenosis), $R_n = R_a = R_M = 0$ (no nanoparticles), N_t, N_b tends to zero (no temperature), $r_1 = 0$, $\gamma^* = \eta^* = \beta^* = 0$ and $\lambda_1 = 0$ is depicted in figure 4-A. Through this figure we have recorded the previous results which have been early obtained by Fung [30]. Also, the special case of ignoring the parameters $R_n = R_a = R_M = 0$ (no nanoparticles), N_t, N_b tends to zero (no temperature), $r_1 = 0$, $\gamma^* = \eta^* = \beta^* = 0$ and $\lambda_1 = 0$ is depicted in figure 4-B. Through this figure, we have recorded the previous results which have been early obtained by Verma and Parihar [11].

Figure 5-A describes the variation of temperature $\theta(r)$ for different values of the thermophoresis parameter N_t. It is observed that the temperature profile decreases with the increase of N_t in the region $0 \le r \le 0.2$. However, increases in the region $0.2 < r \le 0.9$. The variation of temperature profile $\theta(r)$ for different values of the Brownian motion parameter N_b is described in figure 5-B. It is indicated that the Brownian motion parameter N_b and the thermophoresis parameter N_t have qualitatively similar effects on temperature profile. Figure 5-C indicates the variation of temperature $\theta(r)$ for different values of the thermal slip parameter η^*. It is observed that, in the domain $0 \le r \le 0.2$, the temperature profile increases with the increase of η^*. It is also found that, in case of no-slip condition ($\eta^* = 0$), the value of the temperature

profile is lower than that in case of slip condition. Meanwhile, at the complementary of this domain, the inverse occurs. Figure 6-A indicates the variation of the nanoparticle volume fraction in the nanofluid σ vs r-axis for different values of the thermophoresis parameter N_t. It is clear that the nanoparticles phenomena increases with the increase of N_t in the region $0 \le r \le 0.2$. However, this influence decreases in the region $0.2 < r \le 0.8$. Figure 6-B describes the variation of nanoparticle volume fraction in the nanofluid σ vs r-axis for different values of the Brownian motion parameter N_b. It is shown that the Brownian motion parameter N_b and the thermophoresis parameter N_t have qualitatively opposite effects on the nanoparticles phenomena. Figure 6-C indicates the variation of the nanoparticle volume fraction in the nanofluid $\sigma(r)$ for different values of the nanoparticle slip parameter β^*. It is observed that, in the domain $0 \le r \le 0.2$, the nanoparticles phenomena increases with the increase of β^*. It is also found that, in case of no-slip condition ($\beta^* = 0$), the value of nanoparticle volume fraction is lower than that in case of slip condition. Meanwhile, at the complementary of this domain, the inverse occurs. Figures 5-A, 5-B, 5-C, 6-A, 6-B and 6-C show that the temperature profile and nanoparticle phenomena have qualitative similar behavior for slip parameters and Brownian motion parameter. However, they have qualitative opposite behavior for the thermophoresis parameter.

The pressure rise ΔP is plotted vs the mean flow rate for different values of the thermophoresis parameter N_t in figure 7-A. It is observed that with an increase in N_t, the pressure rise decrease. Figure 7-B describes the variation of pressure rise vs the mean flow rate for different values of the Brownian motion parameter N_b. It is observed that the pressure rise increase with the increase of N_b. Furthermore, the peristaltic pumping is defined at the region when ($\Delta P > 0$ and $Q > 0$) (pumping region). It os noticed that the peristaltic pumping region becomes wider as the Brownian motion parameter N_b increases. The pressure rise is plotted vs the mean flow rate for different values of the velocity slip parameter γ^* in figure 7-C. It is found a critical flow rate Q_c at ($Q = 0.5$) approximately. As the domain of the Q becomes ($-0.1 \le Q \le Q_c$), the pressure rise decrease with the increase of γ_*. Also, it is found that the transmission of the curves through a non slip condition ($\gamma^* = 0$) is greater than that through the slip condition ($\gamma^* \neq 0$). Meanwhile, the inverse occurs at the complementary of this domain. Figure 7-D shows the variation of pressure rise vs the mean flow rate for different values of the ratio of relaxation time to retardation one λ_1. It is found that the pressure rise decrease with the increase of λ_1. Also, it is found that the transmission of the curves through a Jeffrey fluid ($\lambda_1 \neq 0$) is greater than that in a Newtonian fluid ($\lambda_1 = 0$). From the pervious figures, it is found that the increase in mean flow rate decreases the pressure rise. Therefore, the maximum flow rate is achieved at zero pressure rise. Also, the maximum pressure rise occurs at zero flow rate. Finally, the relation between pressure rise and mean flow rate is linear.

The friction force of the outer tube ΔF_2 is plotted vs the mean flow rate for different values of the velocity slip parameter γ^* in figure 8-A. It found a critical flow rate Q_c at ($Q = 0.5$) approximately. As the domain of the Q becomes ($-1 \le Q \le Q_c$), the friction force increases with the increase of γ^*. Also, it is found that the transmission of the curves through a non slip condition ($\gamma^* = 0$) is lower than that through the slip condition ($\gamma^* \neq 0$). Meanwhile, the inverse occurs at the complementary of this domain. Figure 8-B shows the variation of friction force vs the mean flow rate for different values of the ratio of relaxation time to retardation one λ_1. It is showed that λ_1 has the same effects as that of γ^* on the friction force. It is noticed that, from these paragraph and previous paragraph, the friction force has the opposite behavior compared to the pressure rise.

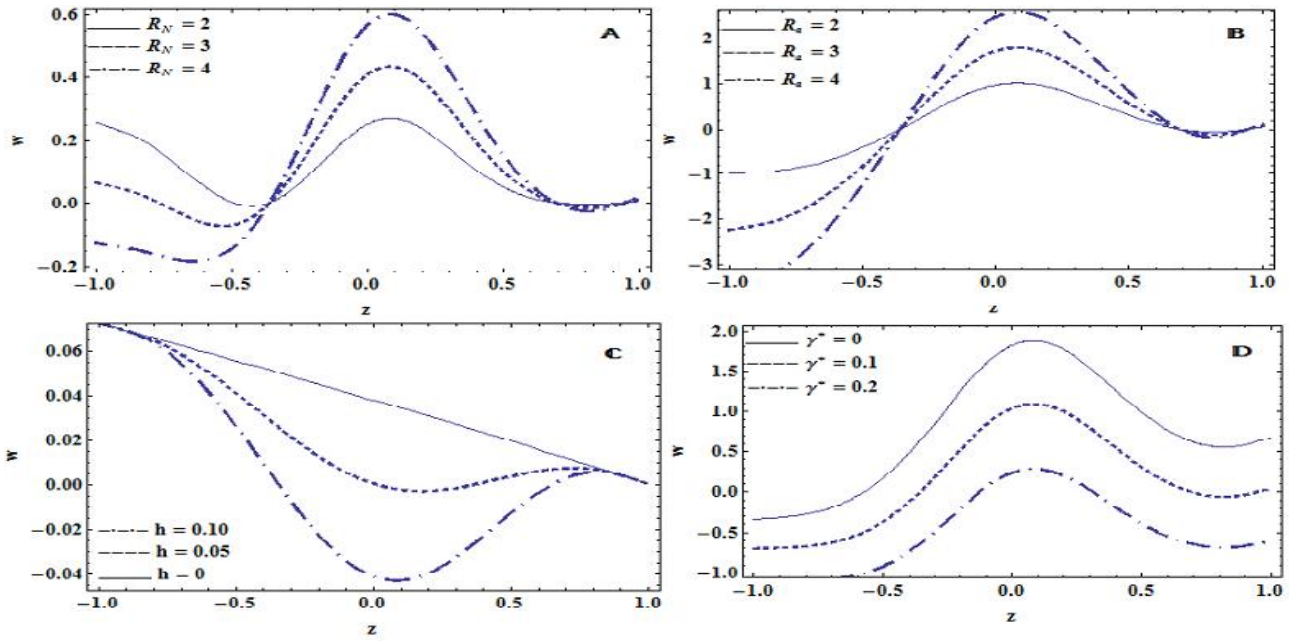

Fig. 2. indicates the variation of the axial velocity w with z -axis for different values of R_N, R_a, h and γ^*

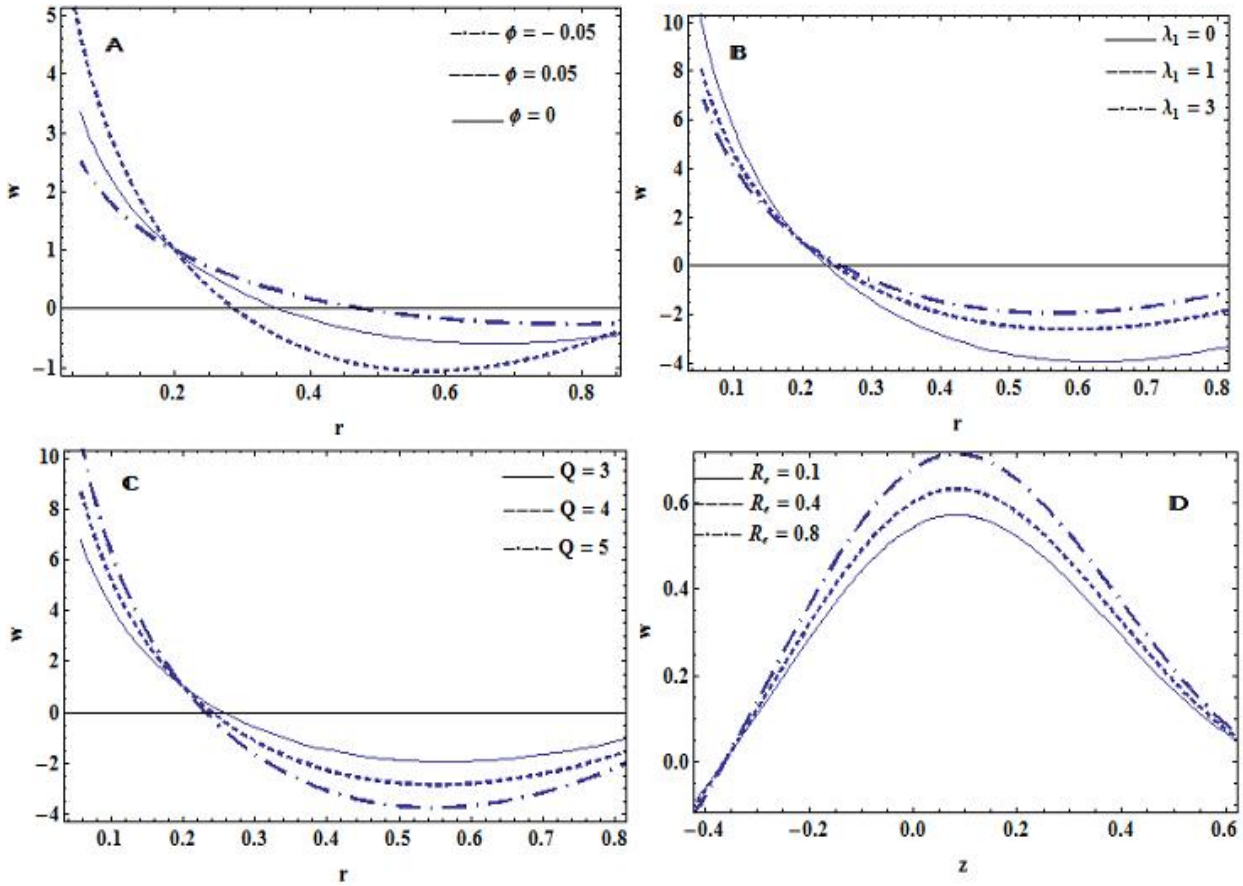

Fig. 3. indicates the variation of the axial velocity w with r -axis for different values of ϕ, λ_1 and Q.

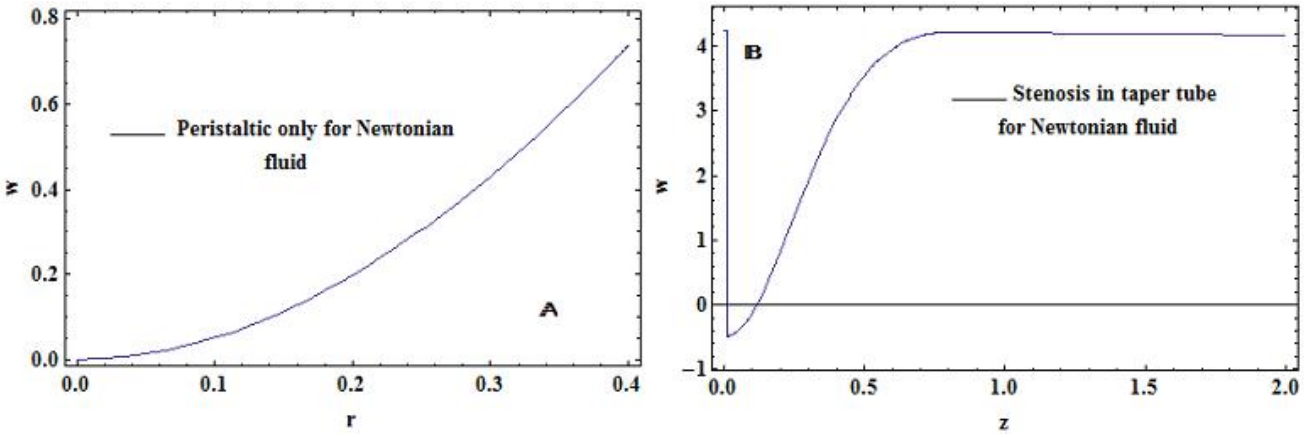

Fig. 4. indicates the axial velocity W for special cases as shown in panels A *and* B*.*

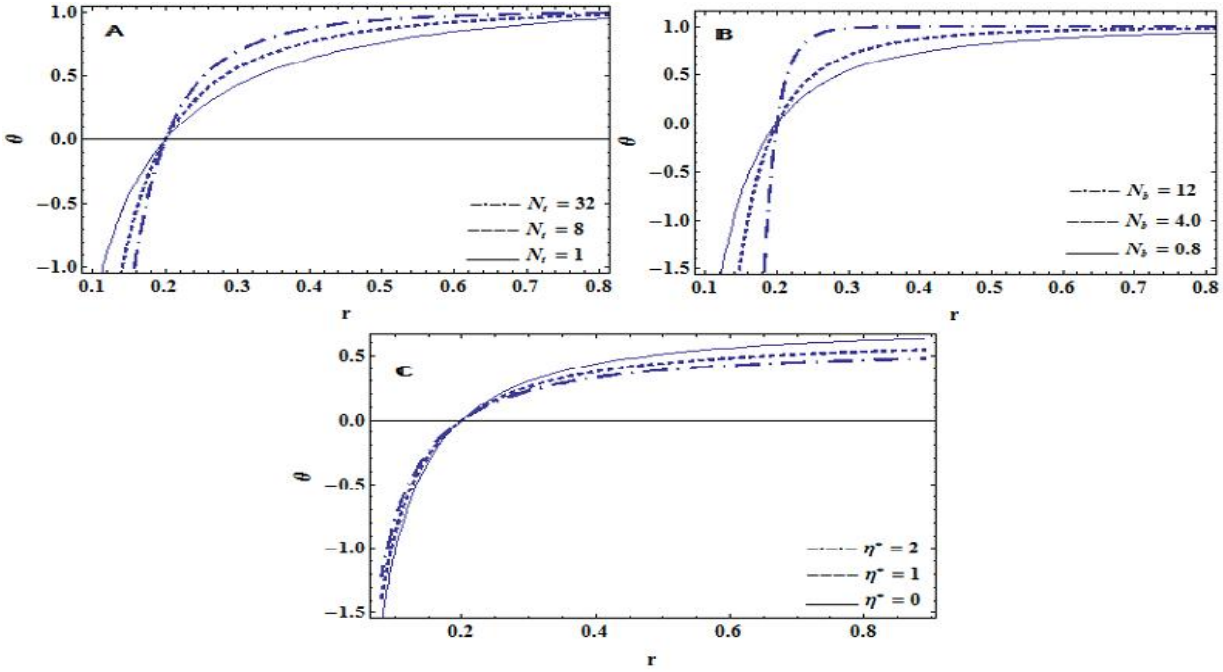

Fig. 5. indicates the variation of the temperature distribution θ with r-axis for different values of N_t, N_b and η^*.

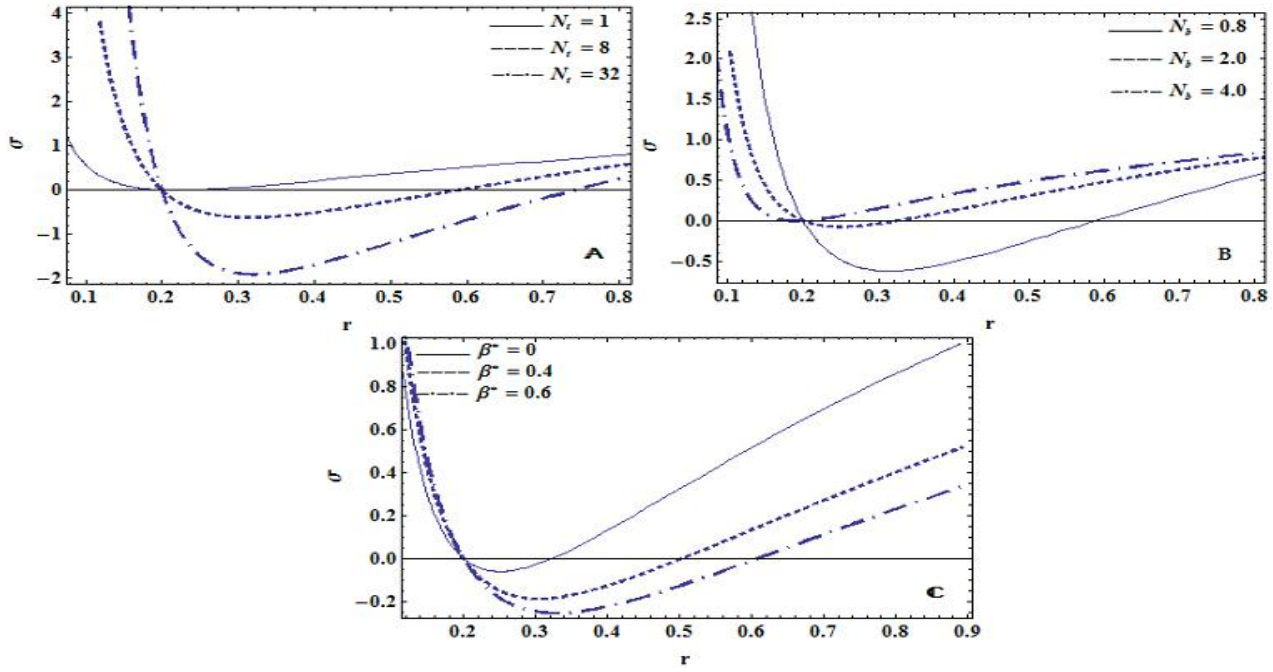

Fig. 6. indicates the variation of the nanoparticle volume fraction in the nanofluid σ with r-axis for different values of N_t, N_b and β^*.

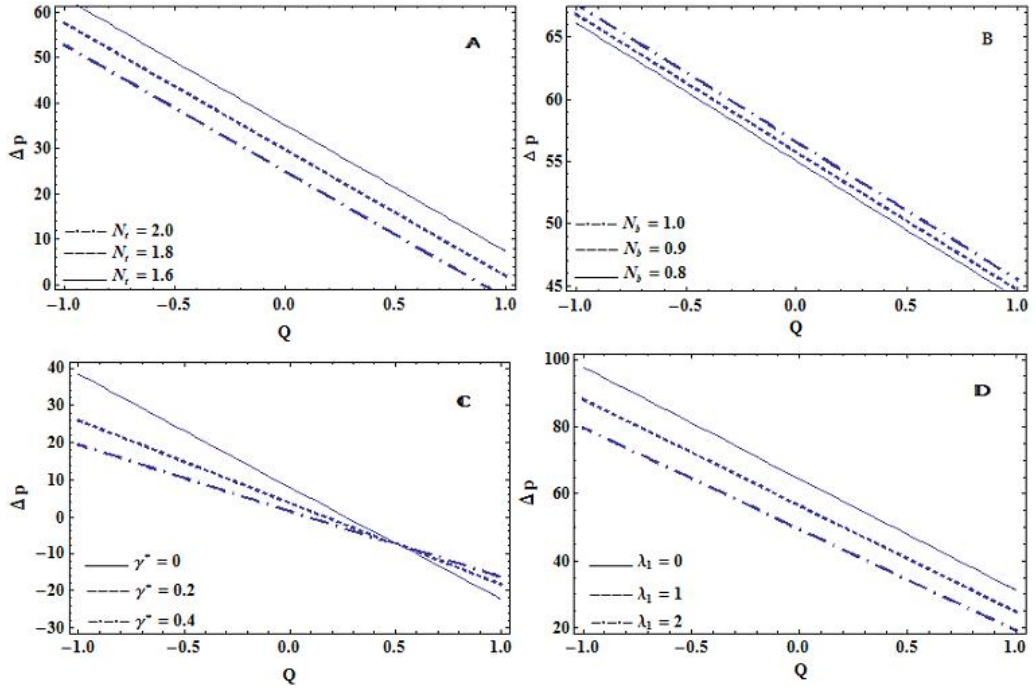

Fig. 7. indicates the variation of pressure rise ΔP vs mean flow rate for different values of N_t, N_b, γ^* and λ_1.

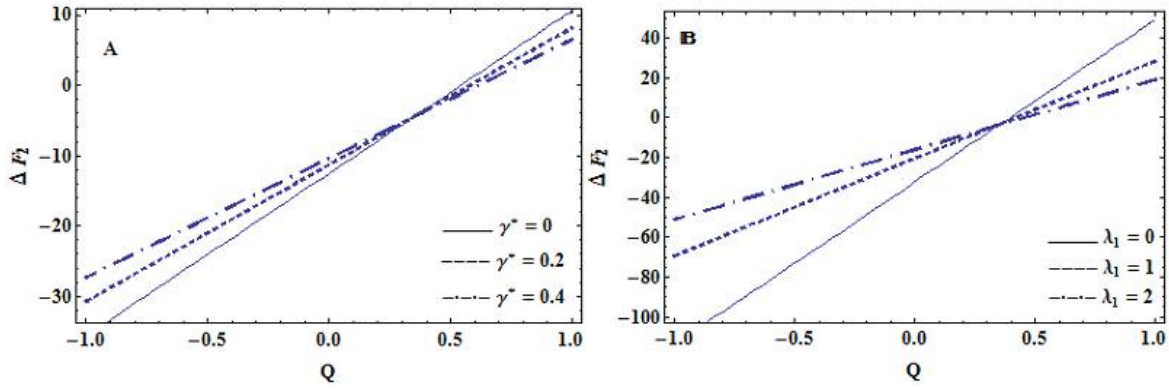

Fig. 8. indicates the variation of friction force of outer tube ΔF_2 vs mean flow rate for different values of γ^* and λ_1.

4.2 TRAPPING

In addition to the pumping phenomenon, trapping is considered as another motivating physical phenomenon in peristaltic motion. As the walls are stationary, trapping phenomenon may be anticipated that the streamlines have a shape similar to the walls. However, in the wave frame, some streamlines under specific conditions may be separated to enclose a bolus of fluid particles in closed streamlines. Therefore, the structure of an internally circulating bolus of the fluid by closed stream lines is defined as a trapping. Furthermore, this trapped bolus is moved forward along with the speed of the peristaltic wave. Also, bolus is defined as a volume of fluid bounded by closed streamlines. In addition, the trapping phenomenon has been discussed by many researchers, such that Shapiro [6] and Jaffrin [32]. The following figures illustrate the stream lines graphes, in the domain $0 \le z \le 2$, for different values of several parameters. The domain $0 \le z \le 0.8$ represents the region of stenosis.

The effect of the of the maximum height of stenosis h on trapping is illustrated in figure 9-A. It is observed that the trapped bolus increases in size by the increasing of h. The effect of the taper angle ϕ is illustrated in figure 9-B. It is indicated that the taper angle ϕ and the the maximum height of stenosis h have qualitatively similar effects on the size of trapped bolus. The effects of the Brownian motion parameter N_b on the trapping are displayed in figure 10-A. It is observed that the bolus decreases in size by the increasing of N_b. The effects of the thermophoresis parameter N_t on the trapping are displayed in figure 10-B. It is indicated that the Brownian motion parameter N_b and the thermophoresis parameter N_t have qualitatively similar effects on the size of trapped bolus. The effect of the of the mean flow rate Q on trapping is illustrated in figure 11-A. It is noticed that the trapped bolus increases in size by the increasing of Q. The effect of the velocity slip parameter γ^* is illustrated in figure 11-B. It is indicated that the velocity slip parameter γ^* and the mean flow rate Q have qualitatively similar effects on the size of trapped bolus.

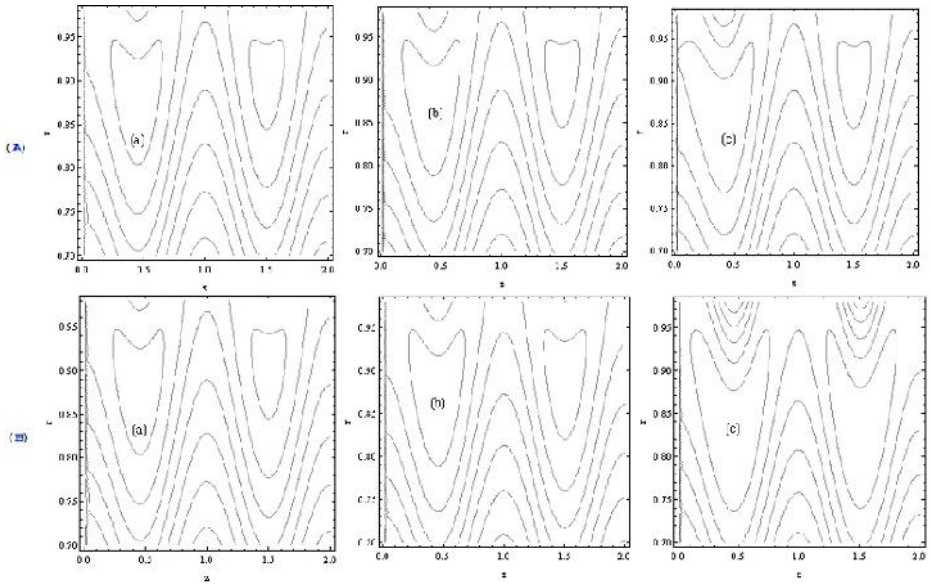

Fig. 9. Streamlines for different values of h and ϕ, respectively.

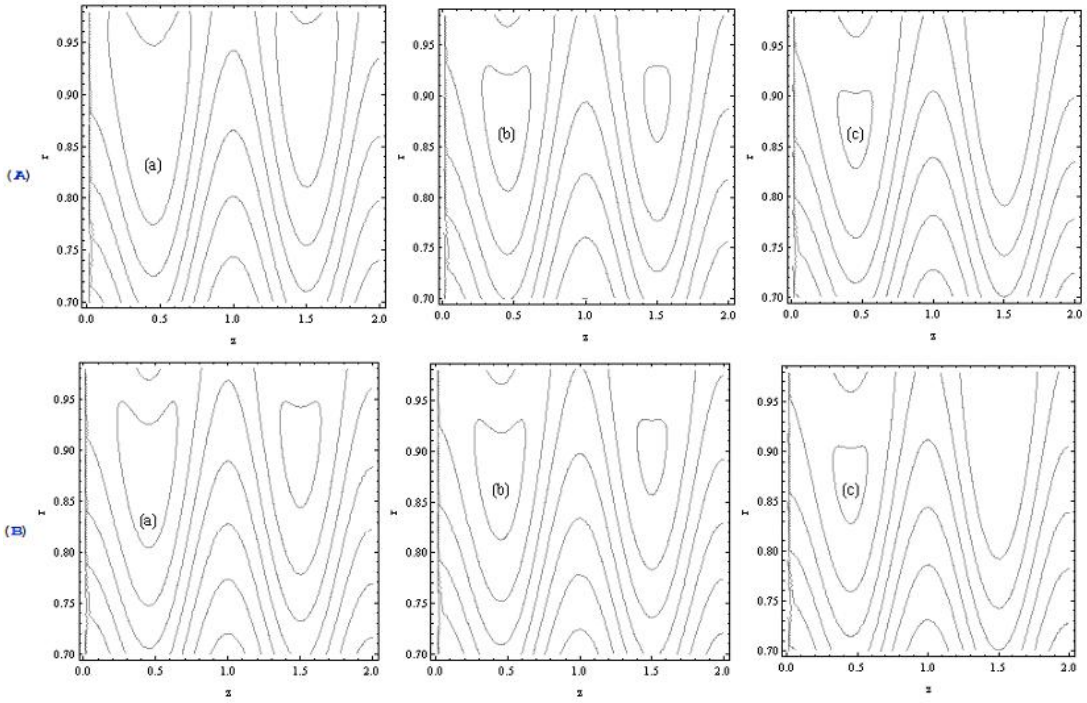

Fig. 10. Streamlines for different values of N_b and N_t, respectively.

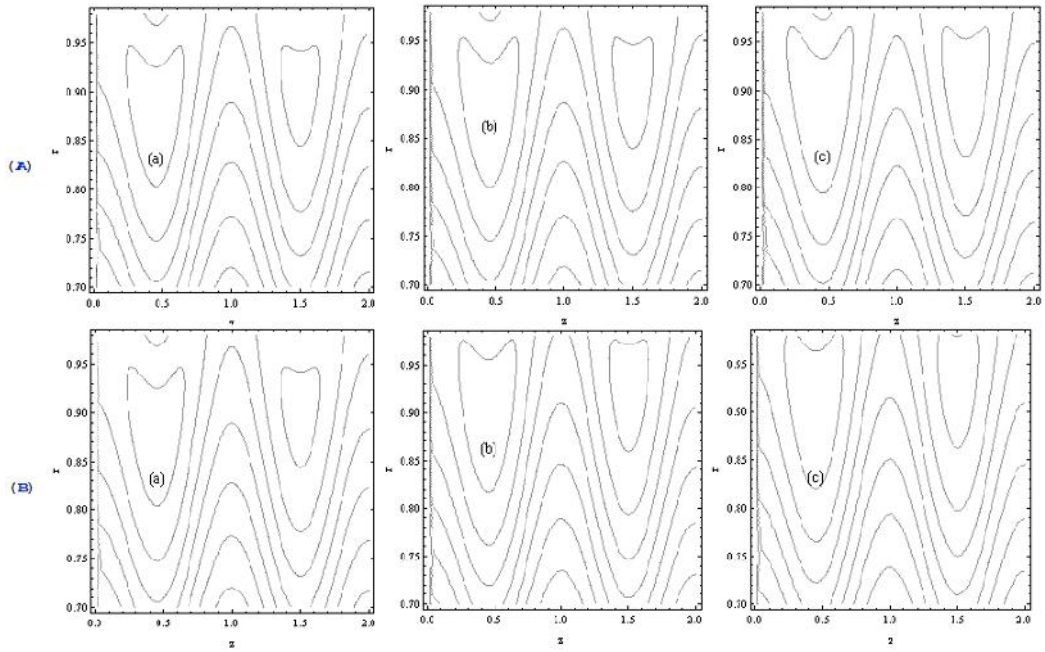

Fig. 11. Streamlines for different values of Q and γ^*, respectively.

5 CONCLUSIONS

In this study we have presented a theoretical approach to investigate the effect of heat transfer on peristaltic flow of Jeffrey nanofluid in a vertical annulus. The flow is streaming through a tapered artery with mild stenosis. Furthermore, the influences of slip conditions of velocity, heat and nanoparticles are also considered. The governing equations of motion, energy and nanoparticle volume fraction are based on a perturbation technique. These equations are analytically solved in accordance with the appropriate boundary conditions. The distributions of velocity, stream function, temperature and nanoparticle are obtained up to the first order. The pressure rise and friction force are obtained in terms of dimensionless flow rate Q by using numerical integration. Numerical calculations are adopted to obtain the effects of several parameters, such as the Reynolds number, the slip parameters, Brownian motion parameter, thermophoresis parameter, the taper angle, nanoparticles Rayleigh number, thermal Rayleigh number, the ratio of relaxation to retardation times and the maximum height of stenosis. Trapping phenomena is also discussed.

The concluding remarks may be drawn as follows:

• Pumping characteristics

(a) As the domain ($-0.4 \le z \le 0.6$), the axial velocity increases with the increase of R_N and R_a. Meanwhile, the inverse occurs at the complementary of this domain.

(b) The axial velocity decreases with the increase of γ^*.

(c) As the domain of the maximum height of stenosis h becomes ($-.8 \le z \le 0.8$), the axial velocity decreases with the increase of h. Meanwhile, at the complementary of this domain, the curves of this velocity are coincide to each others.

(d) The temperature profile decreases with the increase of N_t in the region $0 \le r \le 0.2$. However, it increases in the region $0.2 < r \le 0.9$.

(e) The Brownian motion parameter N_b and the thermophoresis parameter N_t have qualitatively similar effects on temperature profile.

(f) In the domain $0 \le r \le 0.2$, the nanoparticles phenomena increases with the increase of β^*. It is also found that, in case of no-slip condition ($\beta^* = 0$), the value of nanoparticle volume fraction is lower than that in case of slip condition.

Meanwhile, at the complementary of this domain, the inverse occurs.

(g) The values of the pressure rise increases with the increase of N_b.

(h) The increase in mean flow rate decreases the pressure rise. Therefore, the maximum flow rate is achieved at zero pressure rise. Also, the maximum pressure rise occurs at zero flow rate.

(i) There exist a critical flow rate Q_c at ($Q = 0.5$) approximately. As the domain of the Q becomes ($-1 \le Q \le Q_c$), the friction force increases with the increase of γ^*. Meanwhile, the inverse occurs at the complementary of this domain.

(j) The friction force has the opposite behavior compared to the pressure rise.

• **Trapping**

(a) The size of the trapped bolus decreases with the increasing of Brownian motion parameter N_b and thermophoresis parameter N_t.

(b) The size of the trapped bolus increases with the increasing of maximum height of stenosis h, taper angle ϕ and slip parameter γ^*.

To the best of our knowledge, This study is very important in the field of fluid mechanics because it have many applications in many scientific fields such as medicine, medical industrial and others.

Caption of figures

- Figure 2-A is prepared for various values of the parameters: $L = 1$, $d = 2$, $z_0 = 0.8$, $Q = 3$, $r_1 = 0.2$, $N_b = 0.8$, $N_t = 2$, $\gamma^* = \eta^* = \beta^* = 0.1$, $\phi = 0.05$, $h = 0.13$, $\lambda_1 = 5$, $R_a = 2$, $R_M = 2$, $V_0^* = 1$, $R_e = 10$ and ($R_N = 2,3,4$).
- Figure 2-B is prepared for various values of the parameters: $L = 1$, $d = 2$, $z_0 = 0.8$, $Q = 3$, $r_1 = 0.2$, $N_b = 0.8$, $N_t = 2$, $\gamma^* = \eta^* = \beta^* = 0.1$, $\phi = 0.05$, $h = 0.13$, $\lambda_1 = 5$, $R_N = 0.8$, $R_M = 2$, $V_0^* = 1$, $R_e = 10$ and ($R_a = 2,3,4$).
- Figure 2-C is prepared for various values of the parameters: $L = 1$, $d = 2$, $z_0 = 0.8$, $Q = 3$, $r_1 = 0.2$, $N_b = 0.8$, $N_t = 2$, $\gamma^* = \eta^* = \beta^* = 0.1$, $\phi = 0.05$, $R_N = 2$, $\lambda_1 = 5$, $R_a = 0.8$, $R_M = 2$, $V_0^* = 1$, $R_e = 10$ and ($h = 0,0.05,0.1$).
- Figure 2-D is prepared for various values of the parameters: $L = 1$, $d = 2$, $z_0 = 0.8$, $Q = 3$, $r_1 = 0.2$, $N_b = 0.8$, $N_t = 2$, $R_N = 7$, $\eta^* = \beta^* = 0.1$, $\phi = 0.05$, $h = 0.13$, $\lambda_1 = 5$, $R_a = 0.8$, $R_M = 2$, $V_0^* = 1$, $R_e = 10$ and ($\gamma^* = 0,0.1,0.2$).
- Figure 3-A is prepared for various values of the parameters: $L = 1$, $d = 2$, $z_0 = 0.8$, $Q = 3$, $r_1 = 0.2$, $N_b = 0.8$, $N_t = 2$, $\gamma^* = \eta^* = \beta^* = 0.1$, $R_N = 2$, $h = 0.13$, $\lambda_1 = 5$, $R_a = 0.8$, $R_M = 2$, $V_0^* = 1$, $R_e = 10$ and ($\phi = 0,0.05,-0.05$).
- Figure 3-B is prepared for various values of the parameters: $L = 1$, $d = 2$, $z_0 = 0.8$, $Q = 3$, $r_1 = 0.2$, $N_b = 0.8$, $N_t = 2$, $\gamma^* = \eta^* = \beta^* = 0.1$, $\phi = 0.05$, $h = 0.13$, $R_N = 25$, $R_a = 0.8$, $R_M = 2$, $V_0^* = 1$, $R_e = 10$ and ($\lambda_1 = 0,1,3$).
- Figure 3-C is prepared for various values of the parameters: $L = 1$, $d = 2$, $z_0 = 0.8$, $r_1 = 0.2$, $N_b = 0.8$, $N_t = 2$, $\gamma^* = \eta^* = \beta^* = 0.1$, $\phi = 0.05$, $h = 0.13$, $\lambda_1 = 5$, $R_a = 0.8$, $R_M = 2$, $V_0^* = 1$, $R_e = 10$ and ($Q = 3,4,5$).

- Figure 3-D is prepared for various values of the parameters: $L=1$, $d=2$, $z_0=0.8$, $R_N=2$, $r_1=0.2$, $N_b=0.8$, $N_t=2$, $\gamma^*=\eta^*=\beta^*=0.1$, $\phi=0.05$, $h=0.13$, $\lambda_1=5$, $R_a=0.8$, $R_M=2$, $V_0^*=1$, $Q=3$ and ($R_e=0.1,0.4,0.8$).
- Figure 4-A is prepared for various values of the parameters: $L=1$, $d=2$, $z_0=0.8$, ($R_N, r_1, N_b, N_t, \gamma^*, \eta^*, \beta^*, \phi, h, \lambda_1, R_a, R_M, V_0^*$): 0, $Q=3$ and $R_e=10$.
- Figure 4-B is prepared for various values of the parameters: $L=2$, $b=0.01$, $L_0=0.8$, ($R_N, r_1, N_b, N_t, \gamma^*, \eta^*, \beta^*, \lambda_1, R_a, R_M, V_0^*$): 0, $Q=3$, $\phi=0.005$, $h=0.2$ and $R_e=10$.
- Figure 5-A is prepared for various values of the parameters: $L=1$, $d=2$, $z_0=0.8$, $r_1=0.2$, $N_b=0.2$, $\gamma^*=\eta^*=\beta^*=0.1$, $\phi=0.05$, $h=0.1$ and ($N_t=1,8,32$).
- Figure 5-B is prepared for various values of the parameters: $L=1$, $d=2$, $z_0=0.8$, $r_1=0.2$, $N_t=8$, $\gamma^*=\eta^*=\beta^*=0.1$, $\phi=0.05$, $h=0.1$ and ($N_b=0.8,4,12$).
- Figure 5-C is prepared for various values of the parameters: $L=1$, $d=2$, $z_0=0.8$, $r_1=0.2$, $N_t=2$, $N_b=0.8$ $\gamma^*=\beta^*=0.1$, $\phi=0.05$, $h=0.1$ and ($\eta^*=0,1,2$).
- Figures 6-A is prepared for various values of the parameters: $L=1$, $d=2$, $z_0=0.8$, $r_1=0.2$, $N_b=0.8$, $\gamma^*=\eta^*=\beta^*=0.1$, $\phi=0.05$, $h=0.1$ and ($N_t=1,8,32$).
- Figures 6-B is prepared for various values of the parameters: $L=1$, $d=2$, $z_0=0.8$, $r_1=0.2$, $N_t=8$, $\gamma^*=\eta^*=\beta^*=0.1$, $\phi=0.05$, $h=0.1$ and ($N_b=0.8,2,4$).
- Figure 6-C is prepared for various values of the parameters: $L=1$, $d=2$, $z_0=0.8$, $r_1=0.2$, $N_t=2$, $N_b=0.8$ $\gamma^*=\eta^*=0.1$, $\phi=0.05$, $h=0.1$ and ($\beta^*=0,0.4,0.6$).
- Figure 7-A is prepared for various values of the parameters: $L=1$, $d=2$, $z_0=0.8$, $r_1=0.2$, $N_b=0.8$, $R_N=9$ $\gamma^*=\eta^*=\beta^*=0.1$, $\phi=0.05$, $h=0.1$, $\lambda_1=0.4$, $R_a=2$, $R_M=2$, $V_0^*=1$, $R_e=2$ and ($N_t=1.6,1.8,2$).
- Figure 7-B is prepared for various values of the parameters: $L=1$, $d=2$, $z_0=0.8$, $r_1=0.2$, $N_t=1$, $R_N=9$ $\gamma^*=\eta^*=\beta^*=0.1$, $\phi=0.05$, $h=0.1$, $\lambda_1=5$, $R_a=2$, $R_M=2$, $V_0^*=1$, $R_e=2$ and ($N_b=0.8,0.9,1$).
- Figure 7-C is prepared for various values of the parameters: $L=1$, $d=2$, $z_0=0.8$, $r_1=0.2$, $N_b=1$, $R_N=2$ $N_t=3$, $\eta^*=\beta^*=0.1$, $\phi=0.05$, $h=0.1$, $\lambda_1=0.4$, $R_a=2$, $R_M=2$, $V_0^*=1$, $R_e=2$ and ($\gamma^*=0,0.2,0.4$).
- Figure 7-D is prepared for various values of the parameters: $L=1$, $d=2$, $z_0=0.8$, $r_1=0.2$, $N_b=1$, $R_N=9$ $\gamma^*=\eta^*=\beta^*=0.1$, $\phi=0.05$, $h=0.1$, $N_t=3$, $R_a=2$, $R_M=2$, $V_0^*=1$, $R_e=2$ and ($\lambda_1=0,1,2$).
- Figure 8-A is prepared for various values of the parameters: $L=1$, $d=2$, $z_0=0.8$, $r_1=0.2$, $N_b=0.8$, $R_N=2$ $N_t=1$, $\eta^*=\beta^*=0.1$, $\phi=0.05$, $h=0.1$, $\lambda_1=5$, $R_a=2$, $R_M=2$, $V_0^*=1$, $R_e=2$ and ($\gamma^*=0,0.2,0.4$).
- Figure 8-B is prepared for various values of the parameters: $L=1$, $d=2$, $z_0=0.8$, $r_1=0.2$, $N_b=0.8$, $R_N=2$ $\gamma^*=\eta^*=\beta^*=0.1$, $\phi=0.05$, $h=0.1$, $N_t=1$, $R_a=2$, $R_M=2$, $V_0^*=1$, $R_e=2$ and ($\lambda_1=0,1,2$).
- Figure 9-A : Stream lines for $L=2$, $d=2$, $z_0=0.8$, $Q=3$, $r_1=0.2$, $N_b=0.8$, $N_t=1$, $\gamma^*=\eta^*=\beta^*=0.1$,

$\phi = 0.005$, $R_N = 0.8$, $\lambda_1 = 2$, $R_a = 2$, $R_M = 2$, $V_0^* = 1$, $R_e = 10$ and ($h = 0.1, 0.13, 0.17$).

- Figure 9-B : Stream lines for $L = 2$, $d = 2$, $z_0 = 0.8$, $Q = 3$, $r_1 = 0.2$, $N_b = 0.8$, $N_t = 1$, $\gamma^* = \eta^* = \beta^* = 0.1$, $h = 0.1$, $R_N = 0.8$, $\lambda_1 = 2$, $R_a = 2$, $R_M = 2$, $V_0^* = 1$, $R_e = 10$ and ($\phi = 0.005, 0.01, 0.03$).
- Figure 10-A : Stream lines for $L = 2$, $d = 2$, $z_0 = 0.8$, $Q = 3$, $r_1 = 0.2$, $h = 0.1$, $N_t = 2$, $\gamma^* = \eta^* = \beta^* = 0.1$, $\phi = 0.005$, $R_N = 0.8$, $\lambda_1 = 2$, $R_a = 2$, $R_M = 2$, $V_0^* = 1$, $R_e = 10$ and ($N_b = 0.8, 2, 3$).
- Figure 10-B : Stream lines for $L = 2$, $d = 2$, $z_0 = 0.8$, $Q = 3$, $r_1 = 0.2$, $h = 0.1$, $N_b = 0.8$, $\gamma^* = \eta^* = \beta^* = 0.1$, $\phi = 0.005$, $R_N = 0.8$, $\lambda_1 = 2$, $R_a = 2$, $R_M = 2$, $V_0^* = 1$, $R_e = 10$ and ($N_t = 1, 1.2, 1.5$).
- Figure 11-A : Stream lines for $L = 2$, $d = 2$, $z_0 = 0.8$, $N_b = 0.8$, $r_1 = 0.2$, $h = 0.1$, $N_t = 1$, $\gamma^* = \eta^* = \beta^* = 0.1$, $\phi = 0.005$, $R_N = 0.8$, $\lambda_1 = 2$, $R_a = 2$, $R_M = 2$, $V_0^* = 1$, $R_e = 10$ and ($Q = 3, 3.01, 3.03$).
- Figure 11-B : Stream lines for $L = 2$, $d = 2$, $z_0 = 0.8$, $Q = 3$, $r_1 = 0.2$, $h = 0.1$, $N_b = 0.8$, $N_t = 1$, $\eta^* = \beta^* = 0.1$, $\phi = 0.005$, $R_N = 0.8$, $\lambda_1 = 2$, $R_a = 2$, $R_M = 2$, $V_0^* = 1$, $R_e = 10$ and ($\gamma^* = 0.1, 0.18, 0.2$).

REFERENCES

[1] Hayat T., Awais M., Obaidat S., Three-dimensional flow of a Jeffrey fluid over a linearly stretching sheet, Commun. Nonlinear Sci. Numer. Simul., 17 (2012) 699-707.

[2] Vajravelu K., Sreenadh S., Lakshminarayana P., The influence of heat transfer on peristaltic transport of a Jeffrey fluid in a vertical porous stratum, Commun. Nonlinear Sci. Numer. Simul., 16 (2011) 3107-3125.

[3] Lalitha Jyothi K., Devaki P., Sreenadh S., Pulsatile flow of a Jeffrey fluid in a circular tube having internal porous lining, Int. J. Math. Archive, 4 (2013) 75-82.

[4] Latham T. W., Fluid motion in a peristaltic pump, MS Thesis, MIT, Cambridge, M.A., (1966).

[5] Burns J.C., Parkes T., Peristaltic motion, J. Fluid Mech., 29 (1967) 731-743.

[6] Shapiro A. H., Jaffrin M. Y., Weinberg S. L., Peristaltic pumping with long wave lengths at low Reynolds number, J. Fluid Mech., 37 (1969) 799-825.

[7] Manton M. J., Long-wave length peristaltic pumping at low Reynolds number, J. Fluid Mech., 68 (1975) 467-476.

[8] Ang K.C., Mazumdar J.N., Mathematical modeling of three dimentional flow through an asymmetric arterial stenosis, Math. Comput. Modell., 25 (1997) 19-29.

[9] Nichols W. W., Orourke M. F., McDonald's Blood Flow in Arteries, USA by Oxford University Press, Inc., New York, (1973).

[10] Chakravarty S., Datta A., Mandal P.K., Analysis of nonlinear blood flow in a stenosed flexible artery, Int. J. Eng. Sci., 33 (1995) 1821-1837.

[11] Verma N., Parihar R. S., Mathematical model of blood flow through a tapered artery with mild stenosis and hematocrit, J. Mod. Math. Stat., 4 (2010) 38-43.

[12] Srinivas S., Kothandapani M. Peristaltic transport in an asymmetric channel with heat transfer, Int. Comm. Heat Mass Trans. 35 (2008) 514-522.

[13] Arora C. P., Heat and Mass Transfer, 2nd ed., Khanna Publishers, Delhi, (1997).

[14] Nadeem S., Akbar N. S., Influence of heat transfer on a peristaltic transport of Herschel-Bulkley fluid in a non uniform inclined tube, Commun. Nonlinear Sci. Numer. Simulat., 14 (2009) 4100-4113.

[15] Choi S. U. S., Enhancing thermal conductivity of fluids with nanoparticles, developments and applications of non-Newtonian flow, ASME FED 231 (1995) 99-105.

[16] Choi S. U. S., Zhang Z. G., Yu W., Lockwood F. E., Grulke E. A., Anomalous thermal conductivity enhancement in nanotube suspensions, Appl. Phy. Lett., 79 (2001) 2252-2254.

[17] Eijkle J. C. T., van der Berg A., Nanofluidics: what is it and what can we expect from it?, Microfluid Nanofluid 1 (2005) 249-267.

[18] Mekheimer K. S., Abd elmaboud Y., The influence of heat transfer and magnetic field on peristaltic transport of a Newtonian fluid in a vertical annulus: application of an endoscope, Phy. Lett. A, 372 (2008) 1657-1665.

[19] Pankhurst Q.A., Connolly J., Jones S. K., Dobson J., Applications of magnetic nanoparticles in biomedicine, J. Phy. D, 36

(2003) 167-181.
[20] Akram A., Nadeem S., Abdul Ghafoor, Lee C., Consequances of nanofluid on peristaltic flow in asymmetric channel, Int. J. Basic & Appl. Sci., 12 (2012) 75-96.
[21] Ebaid A., Aly E. H., Exact analytical solution of the peristaltic nanofluids flow in an asymmetric channel with flexible walls and slip condition: Application to the cancer treatment, Comput. & Math. Methods in Medicine, 2013 (2013) 1-8.
[22] Ellahi R., Rahman S. U., Nadeem S., Blood flow of nanofluid through an artery with composite stenosis and permeable walls, Appl. Nanosci. 4 (2014) 919-926.
[23] Nadeem S., Ijaz S., Akbar N. S., A theoretical study of Prandtl nanofluid in a rectangular duct through peristaltic transport, Appl. Nanosci. 4 (2014) 753-760.
[24] Pandey S. K., Chaube M. K., Peristaltic transport of a visco-elastic fluid in a tube of non-uniform cross section, Math. Comput. Modell., 52 (2010) 501-514.
[25] Mandal P.K., An unsteady of non-Newtonian blood flow through tapered arteries with a stenosis, Int. J. Nonlin. Mech., 40 (2005) 151-164.
[26] Akbar N. S., Rahman S. U., Ellahi R., Nadeem S., Nanofluid flow in tapering stenosed arteries with permeable walls, Int. J. Thermal Sci., 85 (2014) 54-61.
[27] Tretheway D. C., Meinhart C. D., Apperant fluid slip at hydrophobic microchannel walls, Phys. Fluids, 14 (2002) 9-12.
[28] Ebaid A., Effects of magnetic field and wall slip conditions on the peristaltic transport of a newtonian fluid in an asymmetric channel, Phys. Lett. A, 372 (2008) 4493-4499. Soc., 22 (2014) 143-151.
[29] Abbasi F. M., Hayat T. Ahmad B., Chen G. Q., Slip effects on mixed convective peristaltic transport of copper-water nanofluid in an inclined channel, PLoS ONE 9 (2014) 1-17.
[30] Fung Y. C., Yin F., Peristaltic waves in circular cylindrical tubes, J. Appl. Mech., 36 (1969) 579-587.
[31] Sheu L. J., Linear stability of convection in a viscoelastic nanofluid layer, World Academy of Sci., Engin. & Tec., 5 (2011) 232-238.
[32] Jaffrin M. Y., Inertia and streamline curvature effects on peristalsis pumping, Int. J. Engng. Sci., 11 (1973) 681-699.